



Strong intensification of extreme fire weather in Europe under 3 °C compared to 2 °C global warming

A. Serkan Bayar¹, Joaquim G. Pinto¹, Célia M. Gouveia^{2,3}, and Alexandre M. Ramos¹

¹Institute of Meteorology and Climate Research - Troposphere Research (IMKTRO), Karlsruhe Institute of Technology (KIT), Karlsruhe, Germany

²IDL-Instituto Dom Luíz, Faculdade de Ciências, Universidade de Lisboa, Lisboa, Portugal

³Instituto Português do Mar e da Atmosfera, Rua C do Aeroporto, Lisboa, Portugal

Correspondence: A. Serkan Bayar (serkan.bayar@partner.kit.edu) and Alexandre M. Ramos (alexandre.ramos@kit.edu)

Abstract.

The climate in Europe is warming faster than the global average, raising concerns about how climate change will affect extreme fire events. In this study, we use ERA5-Land reanalysis data and an ensemble of 34 high-resolution regional climate models (RCMs) from the EURO-CORDEX framework to compute the Canadian Forest Fire Weather Index (FWI) and investigate both recent and projected changes in atmospheric conditions favorable for wildfires across Europe. Historical trends (1950-2023) based on ERA5-Land data reveal statistically significant increases in the frequency and intensity of extreme fire weather in regions such as the Iberian Peninsula, Central Europe, and parts of Eastern Europe. All RCM input fields were bias-adjusted prior to FWI calculation using Quantile Delta Mapping, resulting in improved FWI representation relative to raw simulations. Projections based on the bias-adjusted EURO-CORDEX ensemble indicate that future extreme fire weather will become more frequent, more intense, and more widespread across Europe as global warming progresses. The strongest signals are projected for southern Europe, with a northward expansion of fire-prone conditions under higher global warming levels (GWLs). At 3 °C GWL, the spatial extent of robust changes in extreme fire weather metrics nearly doubles compared to 2 °C, with one metric increasing almost fivefold. Relative increases in frequency generally exceed those in magnitude. These changes coincide with rising vapor pressure deficit, suggesting that thermodynamic processes play a key role through atmospheric drying. The projected intensification of extreme fire weather in Europe highlights the growing need for coordinated climate action along with proactive mitigation strategies.

1 Introduction

Wildfires have been part of Earth's history since the emergence of terrestrial plants more than 400 million years ago (Bowman et al., 2009; Scott and Glasspool, 2006). They are an essential component of the Earth system, shaping the evolution and distribution of plant and animal life, as well as influencing key biogeochemical processes (Bowman et al., 2020; He et al., 2019). Fires burn approximately 4 million km² area each year (Chuvieco et al., 2018) and have significant direct and indirect impacts on both global and regional climate through the emission of greenhouse gases and aerosols. Global mean carbon emissions from fires were estimated at 2.2 Pg of C year⁻¹ during the period 1997-2016 (van der Werf et al., 2017), which

corresponds to roughly 21.6% of global CO₂ emissions from fossil fuels in 2024 (Bowman et al., 2020; Friedlingstein et al., 2025).

Satellite-derived data show a nearly 25% decrease in global burned area between 1998 and 2015 (Andela et al., 2017). This decline is primarily concentrated in tropical savannas and grasslands and is largely attributed to agricultural expansion and changes in land cover (Andela et al., 2017). However, despite this decrease in global burned area, global fire emissions have remained relatively stable (Zheng et al., 2021), which is explained by an increase in forest fire emissions across North America and Eurasia where fires release more CO₂ per unit area burned (Jones et al., 2024; Zheng et al., 2021). Moreover, the frequency and magnitude of extreme wildfires more than doubled between 2003 and 2023 (Cunningham et al., 2024), and a significant proportion of extreme fire events occurred under extreme fire weather conditions (Bowman et al., 2017).

Fire weather refers to atmospheric conditions that are conducive to triggering and propagating wildfires (Masson-Delmotte et al., 2021). Numerous fire weather indices based on daily surface weather variables (e.g., temperature, precipitation, relative humidity, and wind) have been developed and applied across different regions (Jolly et al., 2015; Jones et al., 2022). These indices reflect the effects of atmospheric conditions on fuel dryness and subsequent potential fire danger, and are strongly correlated with the magnitude and extent of wildfires, particularly in ecosystems with intermediate moisture availability (Abatzoglou et al., 2018; Bedia et al., 2015; Carvalho et al., 2008; Jolly et al., 2015; Jones et al., 2022). In recent decades, global increasing trends have been observed both in the duration of the fire season and the frequency of these conditions (Jolly et al., 2015; Jones et al., 2022). Under projected global warming, both the frequency and intensity of extreme fire weather are expected to further increase worldwide (Abatzoglou et al., 2019; Bowman et al., 2017; Jones et al., 2022; Masson-Delmotte et al., 2021).

Europe has warmed at twice the global average rate since the 1980s (Copernicus Climate Change Service (C3S) and WMO). Moreover, approximately 70-90% of the continent's land area is projected to shift into different climate zones by the end of the century under high-emission scenario simulations, with a notable tendency toward warmer and drier conditions in the southern and western regions (Bayar et al., 2023). Consistent with this tendency and the expected increase in compound hot and dry events (Masson-Delmotte et al., 2021), extreme fire weather is also projected to increase across much of Europe (Abatzoglou et al., 2019; Jones et al., 2022), with particularly pronounced changes in the Mediterranean region (Fargeon et al., 2020; Ruffault et al., 2020). In addition, growing concern surrounds the impacts of climate change on extreme fire weather in central Europe, an area that is historically less prone to these events. (Carnicer et al., 2022; Miller et al., 2024; Mozy et al., 2021)

Recently, two pan-European scale studies projected widespread increases in extreme fire weather under the impacts of climate change (El Garroussi et al., 2024; Hetzer et al., 2024). Both studies relied on global climate model outputs from the sixth phase of the Climate Model Intercomparison Project (CMIP6) (Eyring et al., 2016) and applied statistical downscaling techniques to reach the target resolution (~31 km in El Garroussi et al. (2024) and ~9 km in Hetzer et al. (2024)). However, since statistically downscaled fields still inherit the climate change signal from driving global climate models (GCMs) and do not incorporate fine-grid scale physical processes, they may not fully capture important regional scale phenomena, such as snow-albedo feedbacks in mountainous regions (Maraun et al., 2017), potentially leading to the breaking of physical consistence and biased results. To address this limitation, dynamically downscaled regional climate models (RCMs) offer



an alternative approach as they refine the large-scale circulation response obtained from GCMs to finer scales by explicitly
 60 simulating sub-GCM grid-scale processes (Giorgi, 2019). Many studies used RCMs from the Coordinated Regional Climate
 Downscaling Experiment - European Domain (EURO-CORDEX) (Jacob et al., 2014) to project fire weather danger across
 Europe in a warming climate, but most of them relied on relatively smaller ensemble sizes (e.g., de Rigo et al., 2017; Galizia
 et al., 2023) and were often limited to specific regions, such as Greece (Rovithakis et al., 2022), France (Fargeon et al., 2020;
 Varela et al., 2019), or the Iberian Peninsula (Bento et al., 2023; Calheiros et al., 2021).

65 To address these research gaps, we use a relatively large ensemble from the EURO-CORDEX framework (Jacob et al., 2014),
 consisting of 34 GCM-RCM chains and assess extreme fire weather danger at a pan-European scale under global warming.
 We focus on the projected changes at 2 °C and 3 °C global warming levels (GWLs) and rely on scenario simulations based
 on the Representative Concentration Pathway (RCP) 8.5. Fire weather is quantified using the Canadian Forest Fire Weather
 Index (FWI) System (Van Wagner, 1987), as it relies solely on daily meteorological input fields and has been shown to perform
 70 well in Europe, especially in the Mediterranean (Carvalho et al., 2008; Jones et al., 2022; San-Miguel-Ayanz et al., 2012;
 Viegas et al., 1999). Prior to calculating projected fire weather danger, model input fields are bias adjusted using quantile delta
 mapping (QDM) (Cannon et al., 2015), with ERA5-Land reanalysis data (Muñoz-Sabater et al., 2021) serving as reference.
 We also investigate subcomponents in the FWI system and the vapor pressure deficit (VPD) to shed light on potential drivers
 of changes in extreme fire weather. The objectives of this study are as follows:

- 75 – Examine the observed climatology of extreme fire weather across Europe and its associated trends since 1950.
- Assess the added value of bias adjustment using QDM in terms of spatial patterns of bias in extreme FWI for the EURO-
 CORDEX multi-model ensemble median.
- Quantify changes in the frequency and intensity of extreme fire weather at 2 °C and 3 °C GWLs, and identify the potential
 drivers underlying these changes based on the bias-adjusted EURO-CORDEX multi-model ensemble.

80 The study is structured as follows: Section 2 gives an overview of data and methods, Section 3 describes the results in detail,
 including the observed trends, the added value of bias adjustment, and projections of extreme fire weather across Europe in a
 warming climate. Section 4 summarizes the main results and provides a discussion.

2 Data and Methods

2.1 Data

85 2.1.1 ERA5-Land Reanalysis

In this study, hourly atmospheric fields, including 2-meter temperature, precipitation, 10 meter u (zonal) and v (meridional)
 components of wind speed and 2-meter dew point temperature were used from the European Centre for Medium-Range
 Weather Forecasts (ECMWF) ERA5-Land reanalysis (Muñoz-Sabater et al., 2021). The main advantage of ERA5-Land is



its enhanced horizontal grid resolution of 9 km, compared to 31 km for ERA5 (Muñoz-Sabater et al., 2021). The dataset covers the period from 1950 to the present, with data up to 2023 used in this study. ERA5-Land reanalysis data were used for several purposes throughout the study, including: 1) the estimation of the most suitable input variable combination to calculate FWI at daily resolution, 2) the calculation of historical climatology and observed trends, and 3) the adjustment of biases in atmospheric fields derived from GCM-RCM chains.

2.1.2 EURO-CORDEX Simulations

We considered a set of 34 GCM-RCM chains from the EURO-CORDEX framework (Jacob et al., 2014) to quantify future changes in extreme fire weather in Europe. The variables used include daily maximum temperature, accumulated precipitation, mean relative humidity, and maximum wind speed (for details on variable selection, see Sections 2.2.4 and 3.1). EURO-CORDEX simulations are dynamically downscaled from GCMs participating in CMIP5 (Taylor et al., 2012) to provide high-resolution regional climate simulations across Europe. All models share a common horizontal grid spacing of ~ 12 km. Both historical simulations (covering the period from 1950 or 1970, depending on the model, to 2005) and scenario simulations (covering 2006 to 2100) were used. The scenario simulations follow the RCP8.5 scenario, which represents a high-end greenhouse gas emission scenario with a radiative forcing of 8.5 W m^{-2} by the end of the century. A single model realization (r1i1p1) was used for each model. All simulations were regridded to the ERA5-Land grid resolution of 9 km using first-order conservative remapping (Jones, 1999). The list of models used in this study is provided in Table 1.

In order to better understand regional differences in extreme fire weather behavior across Europe, these metrics have also been spatially aggregated and averaged over the so-called PRUDENCE regions (Christensen and Christensen, 2007). In addition to the eight regions that were previously defined, Turkey was included as an additional subregion (Figure 1), as it has been shown to be particularly sensitive to extreme climate events (Gumus et al., 2023). Note that the eastern boundary of Turkey is not covered by the EURO-CORDEX domain and is therefore not included in this study.

2.2 Methods

2.2.1 Global Warming Levels

We use GWLs to quantify changes in extreme fire weather as many drivers of global and regional climate impacts are closely linked to GWLs (Masson-Delmotte et al., 2021). GCMs have different climate sensitivities and each follows its own trajectory to reach a given GWL at a different time. Using the GWL approach enables the estimation of impacts independently of the specific scenario or timing of when a given GWL is reached. This study focuses on $+2^\circ\text{C}$ and $+3^\circ\text{C}$ GWLs relative to the preindustrial reference period 1881-1910 following Moemken et al. (2022) and Hundhausen et al. (2024). The methodology is based on the time sampling approach (James et al., 2017) as implemented by Vautard et al. (2014) and Teichmann et al. (2018) for regional climate change signals in Europe.

First, the 30-year running average of the global mean temperature was calculated from the scenario simulations of the GCMs. The observed global warming from 1881-1910 to 1971-2000 was already estimated as 0.46°C (Vautard et al., 2014).



Table 1. List of the 34 GCM-RCM chains used in this study. All scenario simulations follow RCP8.5, so that all models reach the 3 °C GWL during the 21st century. All models belong to the same ensemble member r1i1p1.

GCM	RCM
CNRM-CERFACS-CNRM-CM5 (Voldoire et al., 2013)	CLMcom-ETH-COSMO-crCLIM-v1-1 (Sørland et al., 2021) DMI-HIRHAM5 (Bøssing Christensen et al., 2007) GERICS-REMO2015 (Jacob et al., 2012) IPSL-WRF381P (Vautard et al., 2013) KNMI-RACMO22E (Meijgaard et al., 2012) SMHI-RCA4 (Kjellström et al., 2016)
ICHEC-EC-EARTH (Hazeleger et al., 2012)	CLMcom-ETH-COSMO-crCLIM-v1-1 DMI-HIRHAM5 KNMI-RACMO22E SMHI-RCA4
IPSL-IPSL-CM5A-MR (Dufresne et al., 2013)	DMI-HIRHAM5 GERICS-REMO2015 IPSL-WRF381P KNMI-RACMO22E SMHI-RCA4
MOHC-HadGEM2-ES (Collins et al., 2011)	CLMcom-ETH-COSMO-crCLIM-v1-1 DMI-HIRHAM5 IPSL-WRF381P KNMI-RACMO22E MOHC-HadREM3-GA7-05 (Tinker et al., 2015) SMHI-RCA4
MPI-M-MPI-ESM-LR (Giorgetta et al., 2013)	CLMcom-ETH-COSMO-crCLIM-v1-1 DMI-HIRHAM5 IPSL-WRF381P KNMI-RACMO22E MOHC-HadREM3-GA7-05 SMHI-RCA4
NCC-NorESM1-M (Bentsen et al., 2013)	CLMcom-ETH-COSMO-crCLIM-v1-1 DMI-HIRHAM5 GERICS-REMO2015 IPSL-WRF381P KNMI-RACMO22E MOHC-HadREM3-GA7-05 SMHI-RCA4

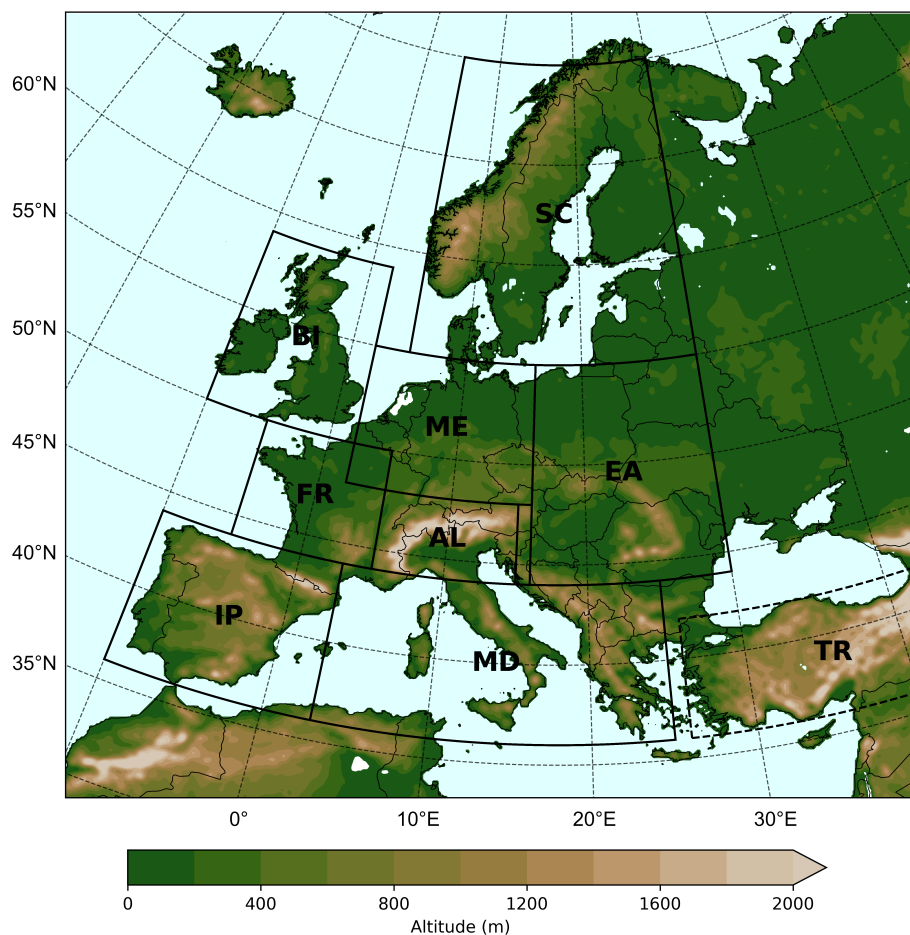


Figure 1. PRUDENCE regions investigated in this study, based on the definitions of Christensen and Christensen (2007) and shown with surface altitude data from COSMO-CLM in the EURO-CORDEX domain (Sørland et al., 2021). BI = British Isles, SC = Scandinavia, FR = France, ME = Mid-Europe, AL = Alps, EA = Eastern Europe, IP = Iberian Peninsula, MD = Mediterranean, TR = Turkey. Note that Turkey is included here in addition to the previously defined regions.

The average global mean temperature of the GCMs during 1971-2000 was then used as historical reference, so that an increase of 1.54 °C (2.54 °C) from that value corresponds to +2 °C (+3 °C) GWL relative to the preindustrial period. Next, 30-year time periods were identified based on when the relevant GWLs are reached for the first time in the running average (as listed in Table B1). Note that although the GWLs are defined relative to the preindustrial period, the change signals presented in this study are expressed relative to the historical reference period (1971-2000, +0.46 °C). This is a deliberate choice, as RCM simulations from the EURO-CORDEX framework only begin after 1950.



2.2.2 Bias Adjustment of EURO-CORDEX Model Outputs

GCMs are known to have systematic biases due to various factors, such as discretization and spatial averaging within grid cells (Teutschbein and Seibert, 2012), inadequate representation of thermodynamic processes (Wehrli et al., 2018), or inaccuracies in simulating atmospheric dynamics (Shepherd, 2014). Since the nested downscaled model is driven by imposed boundary conditions, RCMs also often inherit the biases of their driving GCMs, such as incorrect placement of storm tracks (Giorgi, 2019), and can also introduce their own biases. Therefore, it is common practice to adjust biases in climate model outputs, particularly before using the results for impact modeling (Chen et al., 2021; Dosio and Paruolo, 2011; Hakala et al., 2018; Muerth et al., 2013).

Here we applied the QDM method (Cannon et al., 2015) to adjust the biases in the input fields extracted from EURO-CORDEX simulations, which were then used to calculate the FWI. First, the non-exceedance probabilities of the simulations were calculated over the projected time window:

$$\tau(t) = F_{s,p}^d [x_{s,p}(t)] \quad (1)$$

where $x_{s,p}(t)$ is the projected simulation value of the variable of interest at time step t , $F_{s,p}^d$ is the empirical cumulative distribution function (CDF) of the time series being corrected (in this case, decades) and $\tau(t)$ is the non-exceedance probability associated with time step t and has a range between 0 and 1.

Next, the relative change signal between the projected and historical simulations was calculated:

$$\Delta(t) = \frac{x_{s,p}(t)}{F_{s,h}^{-1}[\tau(t)]} \quad (2)$$

where $\Delta(t)$ is the relative change signal at time step t and $F_{s,h}^{-1}$ is the inverse CDF of the simulation during the calibration period.

Finally, the calculated climate change signal was multiplied by the corresponding reference observation value (from ERA5-Land) at the same quantile during the calibration period:

$$x_{ba}(t) = F_{r,h}^{-1}[\tau(t)] \Delta(t) \quad (3)$$

where $x_{ba}(t)$ is the bias adjusted variable at time step t and $F_{o,h}^{-1}$ is the inverse CDF of the reference data (ERA5-Land) during the calibration period (1971-2000).

Note that the described multiplicative approach was applied to precipitation, mean relative humidity, and maximum wind speed. An additive version of the same method was used for maximum temperature. For further details on the bias adjustment methodology, please see Appendix A.



2.2.3 FWI Calculation

155 We employ the widely used Canadian Forest Fire Weather Index System (Van Wagner, 1987) to calculate the historical and projected distribution of extreme fire weather throughout Europe. It consists of six components. The first three components are fuel moisture codes, namely, Fine Fuel Moisture Code (FFMC), Duff Moisture Code (DMC), and Drought Code (DC) and they represent the dryness of fuels in different layers of the Canadian forest floor (Wotton, 2009). The final three components of the FWI system represent fire behavior: Initial Spread Index (ISI) predicts the potential rate of fire spread based on wind speed and surface fuel dryness, BUI represents the total amount of fuel available for burning and FWI, which results from the combination of the previous two, is a numeric rating of the potential fire intensity (Wotton, 2009).
 160 speed and surface fuel dryness, BUI represents the total amount of fuel available for burning and FWI, which results from the combination of the previous two, is a numeric rating of the potential fire intensity (Wotton, 2009). Figure 2 provides a schematic overview of the calculation flow and the required atmospheric input fields.

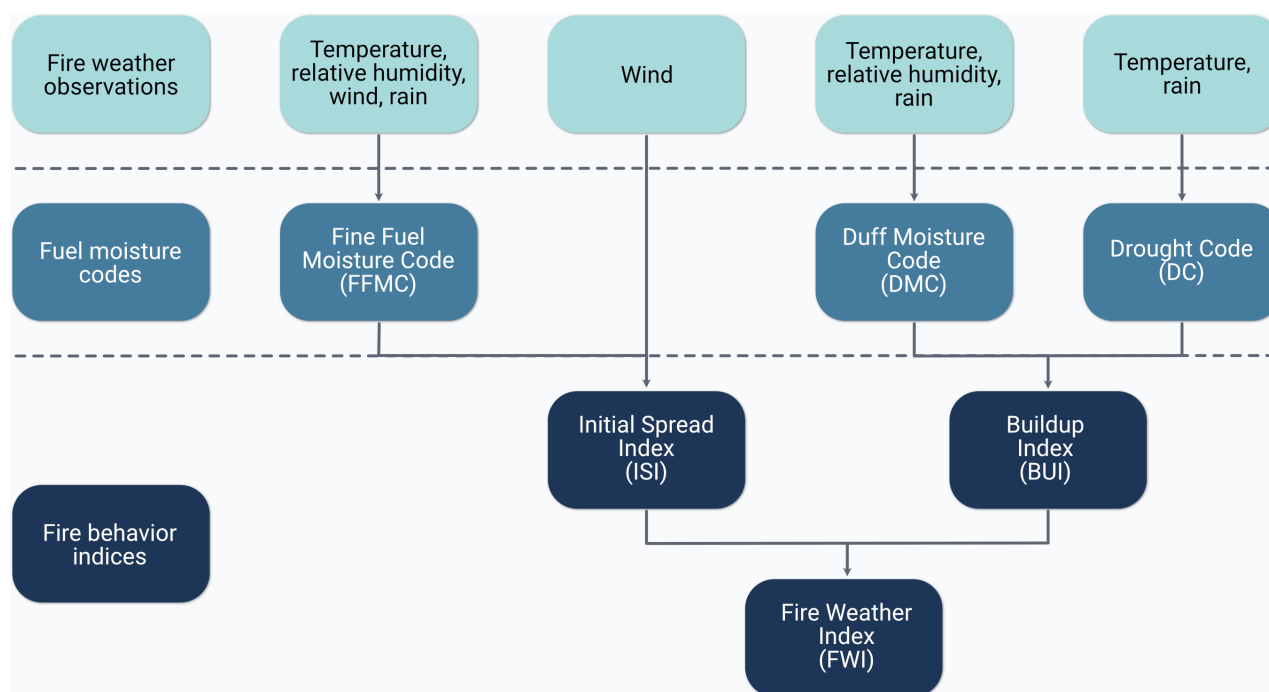


Figure 2. Schematic representation of the Canadian Forest Fire Weather Index System, showing its input variables and six components, based on Van Wagner (1987).

By definition, the FWI calculation requires temperature, relative humidity, and wind speed at local noon (12:00), as well as accumulated precipitation from the previous day's noon to the current day's noon. All input data required for the FWI calculation are directly available from the ERA5-Land reanalysis product, except for relative humidity. Therefore, relative humidity was calculated using the 2-meter temperature and 2-meter dewpoint temperature outputs from ERA5-Land, applying the Magnus formula (Alduchov and Eskridge, 1996). FWI was then computed for the ERA5-Land reanalysis from 1950 to 2023 using these four atmospheric fields at noon as input.



To account for dry conditions outside the fire season (fall and winter), the so-called overwintering approach was applied to the Drought Code (DC) (McElhinny et al., 2020). The overwintering calculation requires a definition of the fire season, outside of which FWI is not calculated. The definition used here follows Wotton and Flannigan (1993), where the fire season begins when the maximum temperature exceeds 12 °C for at least three consecutive days and ends when it drops below 5 °C for at least three consecutive days (Quilcaille et al., 2023). The purpose of overwintering the DC is to capture dry fall and winter conditions, which can lead to more severe fire weather conditions at the beginning of the fire season compared to the default DC value (McElhinny et al., 2020).

2.2.4 Concatenation of the Reanalysis Data and Sensitivity Analysis

In order to account for the variation in local noon times across Europe, three different time zones were used to extract atmospheric fields at the corresponding local noon: UTC+1 for grids west of 0° longitude, UTC+2 for those between 0° and 20°E longitudes and UTC+3 for grids east of 20°E longitude. These three regions were then concatenated into a single product to represent the original FWI calculation.

As many RCMs in the EURO-CORDEX framework do not provide sub-daily information, we searched for the best proxy input combination at daily resolution to approximate the typical noon-time FWI calculation. With this aim, hourly ERA5-Land data were first aggregated to daily resolution, including several combinations (a summary of the daily aggregated variable combinations tested in this study is provided in Table C1). Then, the FWI estimates derived from these combinations were compared with the original noon-time FWI calculation based on ERA5-Land. Specifically, the relative percentage bias in the 95th percentile of FWI was calculated at grid scale to evaluate the performance of each proxy input combination:

$$Bias = \frac{FWI_{comb}^{95} - FWI_{original}^{95}}{FWI_{original}^{95}} \times 100 \quad (4)$$

where $FWI_{original}^{95}$ is the FWI 95th percentile value obtained from the original calculation scheme (noon-time variables), FWI_{comb}^{95} is the FWI 95th percentile value obtained using the input combination being tested. The time period covered is 1950 to 2023.

Finally, the combination resulting in the lowest absolute area-weighted average bias was selected (see Section 3.1). Since some daily resolution atmospheric fields may not be available for some models (e.g., minimum relative humidity), obtaining a sufficiently large model ensemble was also considered in the selection process.

2.2.5 FWI Metrics and Vapor Pressure Deficit

We used four annual FWI metrics to analyze the extreme fire weather behavior at each grid cell for the reference period (1971-2000, +0.46 °C) and at +2 °C and +3 °C GWLs, following the metrics used in Jolly et al. (2015), Abatzoglou et al. (2019) and Quilcaille et al. (2023):



1. Number of days exceeding the reference period (1971-2000) 95th percentile of FWI (FWI_{95d}), representing days with potentially high fire danger at the local scale
2. Number of days exceeding the mid-range value (FWI_{mid} , mean of 30-year averaged annual minimum and maximum FWI during 1971-2000) of FWI (FWI_{fws}), as an indicator of the duration of the fire season
3. 30-year averaged annual maximum FWI (FWI_{max}), as an indication of the magnitude of the local extreme fire danger
4. Annual peak 90-day average FWI (FWI_{fs}), representing the average fire weather conditions during the peak fire season.

To shed light on the potential drivers of changes in extreme fire weather, we further investigate changes in the VPD. VPD is defined as the difference between the saturation vapor pressure (e_s) and the actual vapor pressure (e_a) and serves as an indicator of atmospheric aridity (Seager et al., 2015). It is an essential metric for understanding how atmospheric conditions influence fuel dryness (He et al., 2025) and has been shown to be closely linked to wildfire activity, for example, in western U.S. forests (Abatzoglou and Williams, 2016; Williams et al., 2019). VPD can be calculated using temperature and relative humidity:

$$VPD = e_s(T_a)(1 - RH/100) \quad (5)$$

where RH is the relative humidity and $e_s(T_a)$ is the saturation vapor pressure as a function of the air temperature T_a , calculated using the Clausius-Clapeyron equation:

$$e_s(T_a) = e_s(T_0) \cdot \exp\left(\frac{L_v}{R_v} \left(\frac{1}{T_0} - \frac{1}{T_a}\right)\right) \quad (6)$$

where $e_s(T_0) = 6.112$ hPa is the saturation vapor pressure at the reference temperature $T_0 = 273.15$ K, $L_v = 2.5 \times 10^6$ J kg⁻¹ is the latent heat of vaporization for water and $R_v = 461$ J kg⁻¹ K⁻¹ is the specific gas constant for water vapor. Note that daily maximum temperature and mean relative humidity were used here to estimate VPD, which leads to a possible overestimation (He et al., 2025). However, the focus of this study is not on absolute VPD values, but rather on deviations from the baseline, which minimizes the implications of possible shortcomings.

2.2.6 Significance and Robustness

To calculate trends in the historical period, the non-parametric Theil-Sen slope estimator was used, as it is relatively insensitive to outliers (Sen, 1968; Theil, 1950). The significance of these trends was tested using the non-parametric Mann-Kendall test (Kendall, 1955; Mann, 1945) at a significance level $p < 0.05$.

To assess the robustness of the future climate change signal in the FWI indices, a criterion based on model agreement in both the significance and sign of the reported change was applied. Specifically, the climate change signal is considered robust only when at least 66% of the models agree on both the sign and the statistical significance of the change (Jacob et al., 2014; Pfeifer et al., 2015). The significance of the simulated change was evaluated using a paired t-test at a significance level of $p < 0.05$.



3 Results

3.1 Sensitivity to Different Input Data

The typical FWI calculation is performed using the relevant atmospheric fields at local noon-time (Van Wagner, 1987). Since
 230 many RCMs do not provide subdaily scale information, daily fields need to be identified in such a way that they can replace
 the typical noon-time calculation with minimal bias. Figure 3 shows the distribution of the relative percentage bias in the 95th
 percentile of FWI calculated using the four different input combinations (given in Table C1) relative to the typical noon-time
 95th percentile of FWI ($FWI_{original}^{95}$) across Europe based on ERA5-Land reanalysis (note that the straight lines at 0° and
 20° longitudes result from the concatenation operation described in Section 2.2.4). At the European scale, combinations
 235 that include mean relative humidity generally underestimate extreme fire weather danger (Figures 3a and 3b), while those that
 include minimum relative humidity tend to overestimate it (Figures 3c and 3d).

Since maximum temperature and daily precipitation are common in all combinations, using mean values for both relative
 humidity and wind leads to a substantial underestimation of $FWI_{original}^{95}$ with a mean absolute relative bias of 34.5% (Figure
 3b). In contrast, using daily extremes, i.e., minimum relative humidity and maximum wind speed, considerably overestimates
 240 $FWI_{original}^{95}$, resulting in a mean absolute relative bias of 43.8% (Figure 3c). Thus, using the daily extreme for one variable and
 the mean for the other appears to offer a balanced compromise. The mean absolute biases for these combinations are similar:
 21% for Comb-1 and 20.5% for Comb-4 (Figures 3a and 3d). Selecting Comb-4 would significantly reduce the number of
 models in the EURO-CORDEX ensemble, as minimum relative humidity is not an available output for most simulations.
 Therefore, Comb-1 is selected to calculate the FWI projections using the EURO-CORDEX ensemble, namely, daily maximum
 245 temperature, daily accumulated precipitation, mean relative humidity, and daily maximum wind speed. The remainder of the
 analysis in this study uses these atmospheric fields, for both ERA5-Land reanalysis and EURO-CORDEX models to ensure
 consistency.

3.2 Observed Climatology and Trends

To better understand the influence of ongoing climate change on fire danger in Europe, this section explores the climatology
 250 and trends of two FWI metrics, namely FWI_{mid} and FWI_{95d} , for the period 1950–2023 based on ERA5-Land data. We begin
 with FWI_{mid} , first presenting its climatology (Figure 4a) followed by the corresponding trends (Figure 4c). The FWI_{mid}
 displays a latitudinal gradient, with the highest values found around the Mediterranean Basin due to hot and dry summers,
 while the lower values are found in northern Europe. The Iberian Peninsula and Turkey are mainly associated with FWI_{mid}
 values in the range of moderate and high levels of fire risk according to the scale developed by San-Miguel-Ayanz et al. (2012).
 255 FWI_{mid} shows a positive trend (statically significant) in the central Iberian Peninsula, France and Germany, with statistically
 significant trends observed in 29% of the study domain (Figure 4c). Most of Europe shows an increase in the intensity of fire
 weather conditions, but in eastern Europe and Scandinavia the trends are generally not statistically significant.

FWI^{95} climatology (Figure 4b) displays the highest values in the Mediterranean Basin, with a latitudinal gradient across
 Europe except for lower values in mountainous regions. FWI^{95} values above 38 indicate very high fire danger (San-Miguel-

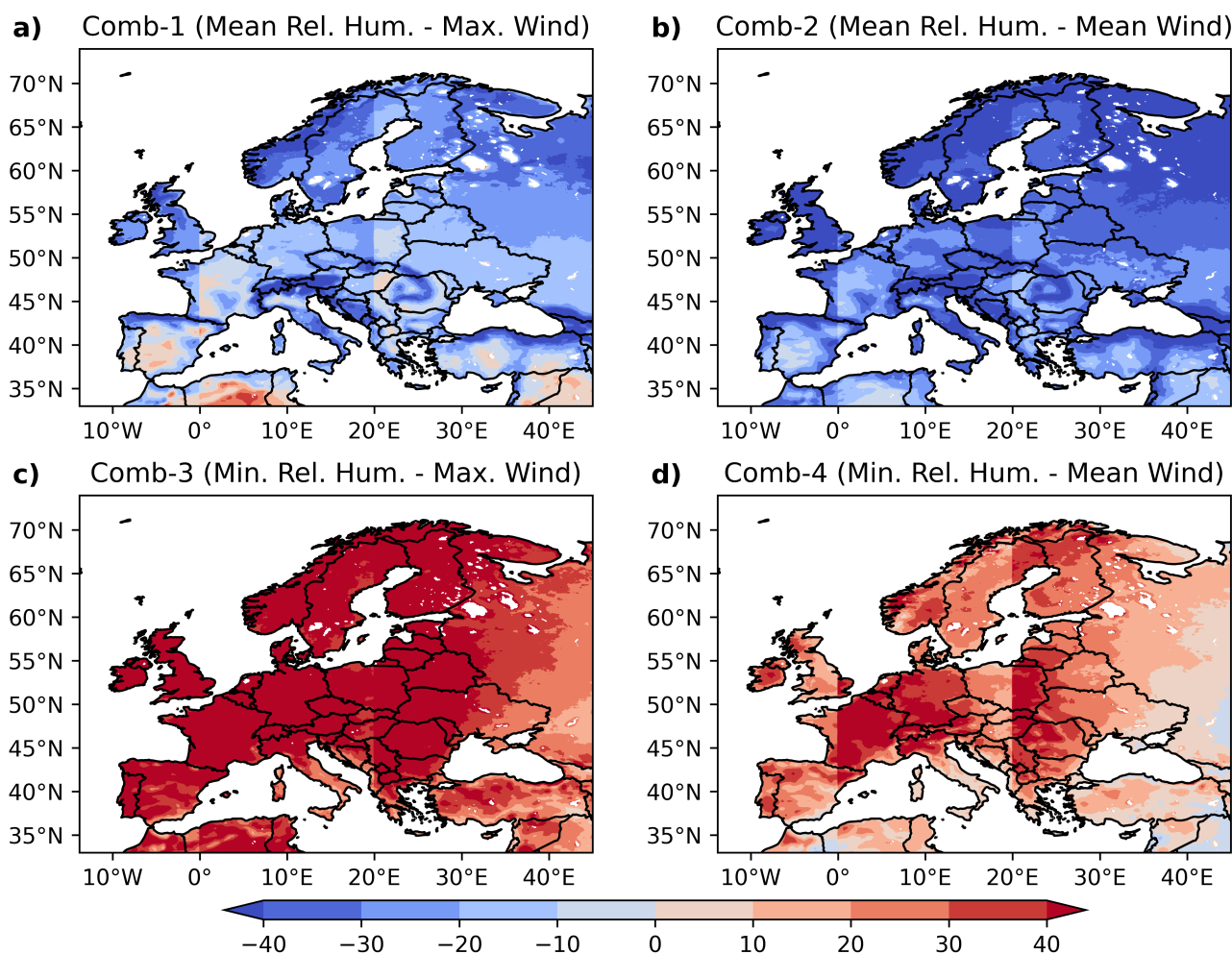


Figure 3. Relative percentage bias of the 95th percentile of FWI calculated using the four input variable combinations **a)** Comb-1, **b)** Comb-2, **c)** Comb-3, and **d)** Comb-4, compared to the original noon-time FWI calculation based on ERA5-Land reanalysis data. Daily maximum temperature and daily precipitation are common to all combinations. The time period analyzed is 1950-2023. Note that the artifacts near 0° and 20° longitudes result from the concatenation operation described in Section 2.2.4. Details of the variables used in all combinations are given in Table C1.

260 Ayanz et al., 2012), but this relationship varies regionally: higher values (~ 50) usually signal extreme danger in warm and dry climates, while lower values (~ 25) may indicate similar danger in cooler and moister climates (Kudláčková et al., 2024). Therefore, FWI_{mid} and FWI^{95} should be interpreted with caution, taking into account the local climate and biome.

Regarding possible trends in the FWI_{95d} (Figure 4d), nearly 37% of all grid cells exhibit a significant trend, almost all of which indicate an increase. Notable positive trends were observed in the Iberian Peninsula, France, Germany and Ukraine, with
 265 trends exceeding $0.3 \text{ days year}^{-1}$, corresponding to more than 20 additional days of extreme fire weather over the 74-year study



period. Some areas of the Iberian Peninsula show trends above $0.5 \text{ days year}^{-1}$, amounting to nearly 40 extra days. In contrast, a small region in the eastern Mediterranean shows a statistically significant negative trend, and some parts of Scandinavia show negative but non-significant changes. Other fire-prone regions, including Italy, the Balkans, and the eastern Mediterranean, show mixed and generally non-significant trends, reflecting large interannual variability in extreme fire weather conditions.

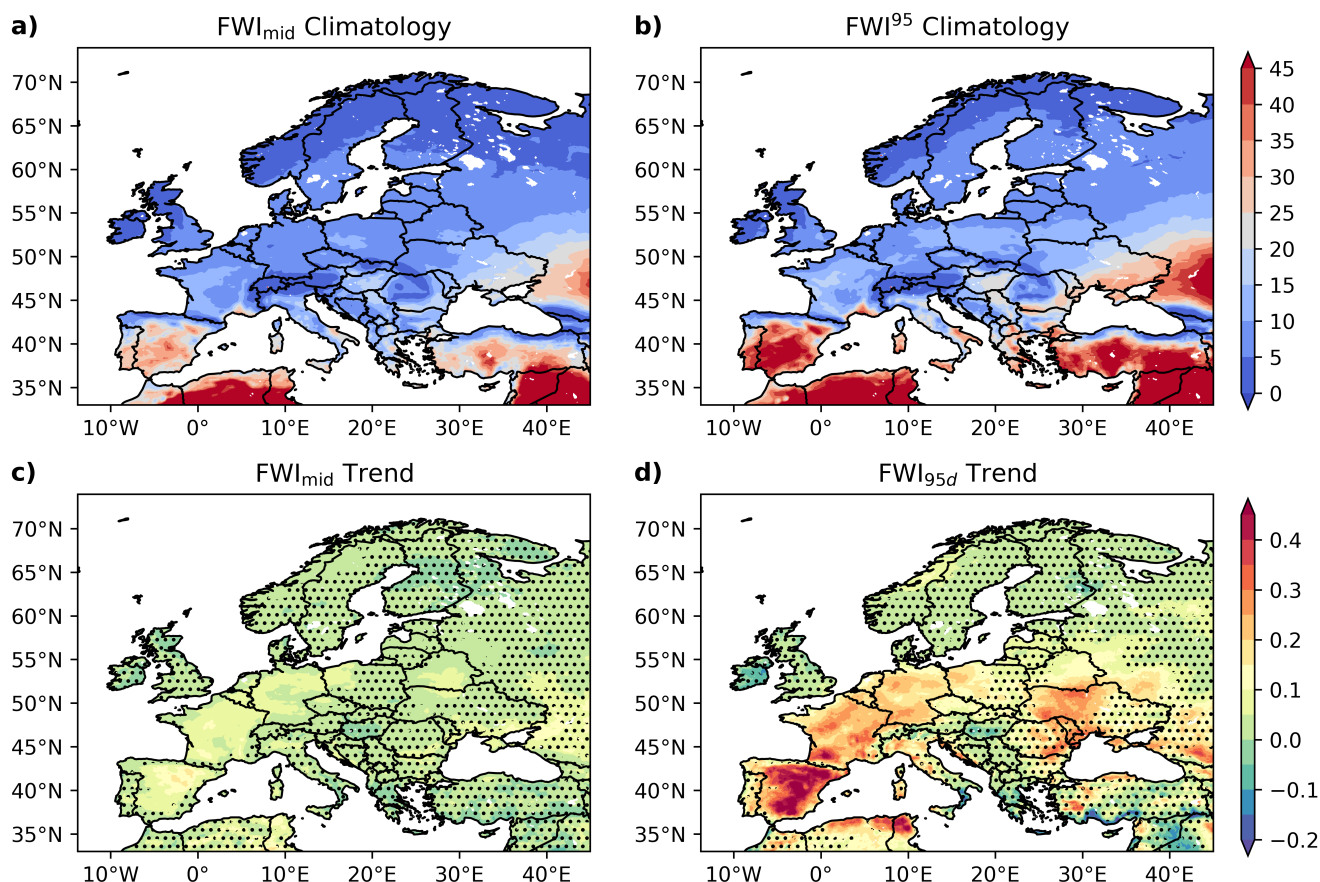


Figure 4. **a)** Observed climatology of the mid-range FWI (FWI_{mid}) and **b)** the 95th percentile FWI (FWI^{95}) during the analysis period of 1950-2023 based on ERA5-Land reanalysis data. **c)** Observed trends (unitless year^{-1}) in FWI_{mid} and **d)** in the number of days per year when FWI exceeds the 95th percentile (FWI_{95d}) relative to the reference period 1971-2000 (days year^{-2}) based on ERA5-Land reanalysis data. Trends are calculated using the Theil-Sen slope estimator. Areas with stippling indicate regions where the trend is not statistically significant ($p < 0.05$), according to the Mann-Kendall test. The analysis covers the period 1950-2023. Note that a single colorbar is used for both trend panels, although the units differ.



270 3.3 Evaluation of Model Performance after Bias Adjustment

GCMs are known to exhibit systematic biases for various reasons, and RCMS often inherit these biases because they use GCMs as boundary conditions for downscaling and may also introduce their own biases (Giorgi, 2019). Figure 5 evaluates the bias in the 95th percentile of the FWI for the EURO-CORDEX ensemble median before and after bias adjustment, relative to the ERA5-Land reanalysis. Note that the time period for the evaluation here is the same as the calibration period for bias adjustment (1971-2000). Although the performance of bias adjustment methods is typically evaluated using a separate validation period (e.g., Cannon et al., 2015), we focus on evaluating model performance during the calibration period as the historical simulations are not long enough to allocate a separate validation period for most of the EURO-CORDEX models, considering that 30 years of data have already been used for calibration. In addition, it is important to note that a cross-validation strategy may not always provide reliable results when evaluating the bias adjustment performance, as the internal variability of the climate system can dominate the differences between calibration and validation periods, potentially leading to misleading evaluations, particularly in mid-latitudes (Maraun and Widmann, 2018).

Adjusting the biases of the individual model input fields prior to the calculation of the FWI results in a significant reduction in the bias of the FWI ensemble median (Figure 5). The spatial mean of the absolute relative percentage bias is 78.2% before adjustment (Figure 5a), with particularly large biases found south of the 50° latitude and in Norway. After bias adjustment, this spatial mean bias of the ensemble median is reduced to 8.6% (Figure 5b), with significant improvements observed in regions where the raw ensemble median previously exhibited large biases. However, some small areas still exhibit high biases, especially mountainous regions, such as parts of the Alps, Carpathians, and Caucasus Mountains (note that the FWI values over the mountainous regions are already very low, so even large percentage biases are also usually low in terms of absolute values). For the purposes of this study, the substantial improvement in model performance by adjusting the input fields with the univariate QDM approach is considered sufficient; hence, the bias-adjusted ensemble is used for the rest of the study.

3.4 Projections of Extreme Fire Weather in Europe

As significant trends in extreme fire weather have been observed in many regions of Europe, and since all regions are projected to experience warmer summer climates, with a particular tendency towards increased drying in the southern and western regions (Bayar et al., 2023), it is reasonable to expect further changes in a warming climate. Figure 6 shows the patterns of the frequency-based FWI metrics (left panels for $FWI_{f_{wsl}}$ and right panels for FWI_{95d}) over Europe during the reference period (1971-2000) and the changes relative to the reference period at 2 °C and 3 °C GWL based on the ensemble median of 34 bias-adjusted EURO-CORDEX models. The climatological patterns of $FWI_{f_{wsl}}$ (Figure 6a) show longer fire seasons in southern Europe, particularly in the Iberian Peninsula, southern Italy, Greece and Turkey, with more than 60 days year⁻¹. In contrast, central and northern Europe experience shorter fire seasons. Since these values may seem lower than expected, it is important to distinguish between different methods for calculating the duration of the fire season. Wotton and Flannigan (1993) define the fire season based on a temperature threshold, and it is used for overwintering the DC (McElhinny et al., 2020; Quilcaille et al., 2023). However, this definition may lead to an overestimation of fire season length, especially in southern

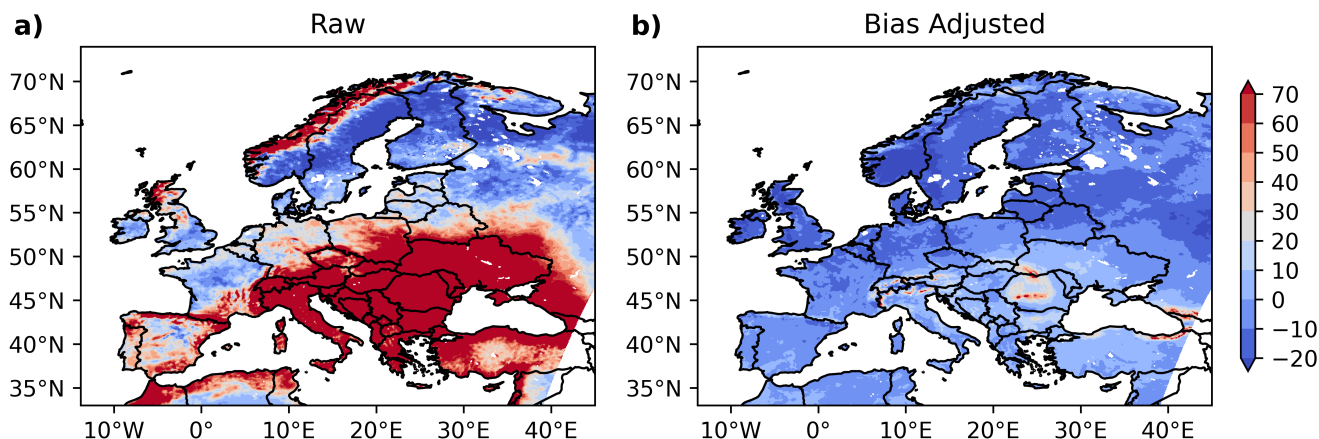


Figure 5. Relative percentage bias (%) in the 95th percentile of FWI for EURO-CORDEX ensemble median relative to ERA5-Land data during 1971-2000, based on **a)** raw and **b)** bias-adjusted simulations.

Europe due to warmer temperatures throughout the year. In contrast, Jolly et al. (2015) define FWI_{fws} as the number of days when FWI exceeds its mid-range value. Here, the definition of Jolly et al. (2015) is followed for FWI_{fws} , as in some other
 305 studies (Abatzoglou et al., 2019; Jones et al., 2022). However, this approach possibly underestimated the actual FWI_{fws} in some regions, because overwintering the DC reduces the number of days with an available FWI value throughout the year due to the condition of Wotton and Flannigan (1993).

The projected changes in FWI_{fws} at 2 °C and 3 °C GWLs relative to the reference period are shown in Figures 6c and 6e, respectively. At 2 °C, robust increases in FWI_{fws} are already evident in some regions, with a magnitude of up to 100%
 310 in areas like parts of the Balkans, but the larger changes are mostly limited to regions with smaller climatological values. The increase in FWI_{fws} becomes more widespread and intense at 3 °C, particularly in France and Balkans, with a relative increase exceeding 150%. Almost all regions show positive changes in FWI_{fws} at both GWLs (except for a small area in northern Poland at 2 °C). The projected mean relative change in FWI_{fws} for the grids where the models agree on both the sign and significance of the change almost doubles between the two GWLs: 49% at 2 °C and 90% at 3 °C. The signal is largely
 315 confined to regions south of 50° latitude, with a robust signal simulated in 27% and 49% of the land area, at 2 °C and 3 °C, respectively.

The right column of Figure 6 shows the number of days per year that exceed the 95th percentile FWI (FWI_{95d}) during the reference period (Figure 6b), along with the relative changes compared to the reference period at 2 °C (Figure 6d) and 3 °C (Figure 6f) GWLs. Here, it is important to note that the spatial distribution of FWI_{95d} during the reference period would be
 320 nearly uniform with around 18 days year⁻¹ across the domain if FWI was calculated continuously, since the 95th percentile is calculated locally for each grid. However, this is not the case here, as overwintering of the DC interrupts the continuous FWI calculation. Therefore, the latitudinal differences in FWI_{95d} are a natural consequence of this calculation. More days exceed

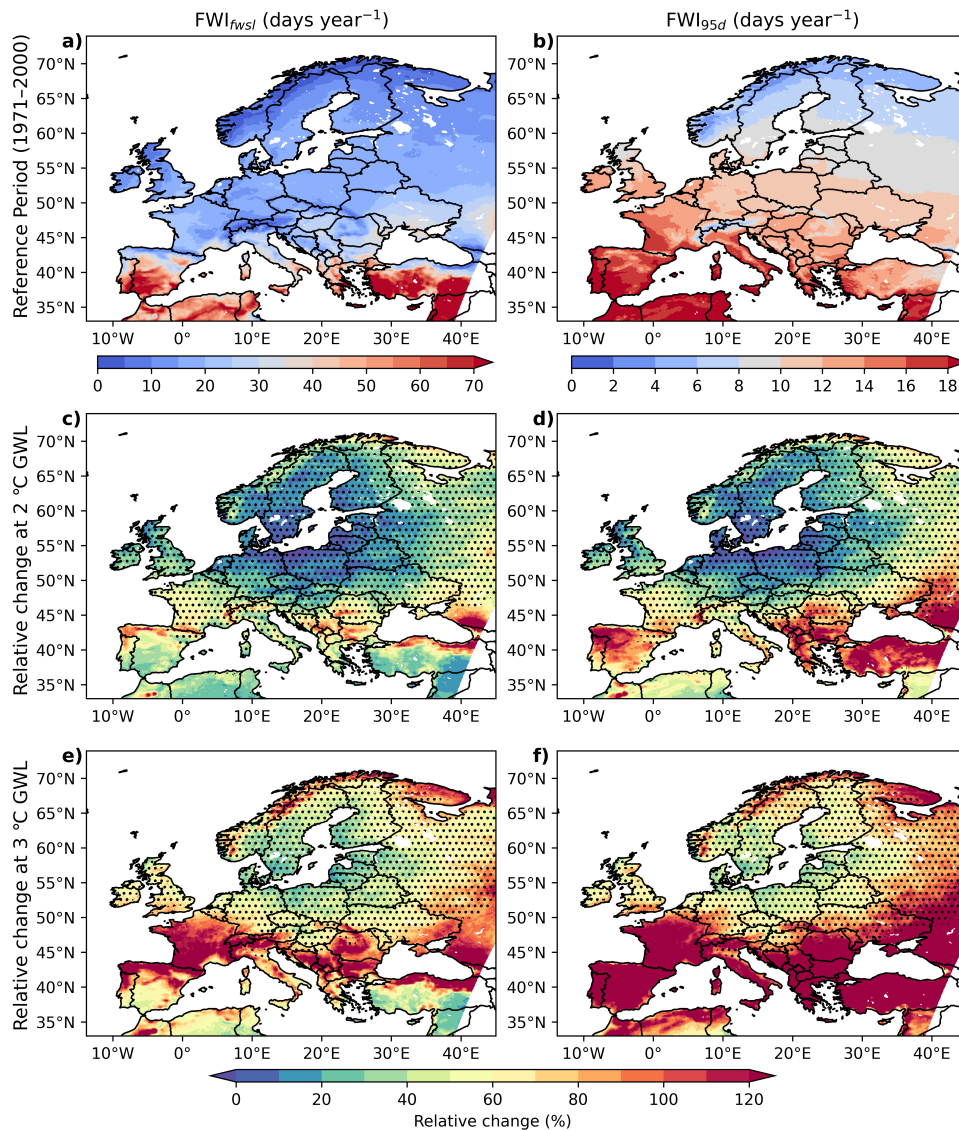


Figure 6. Patterns of frequency-based extreme fire weather metrics and their projected changes in Europe based on the ensemble median of 34 bias-adjusted EURO-CORDEX models. The left panels show the fire weather season length (FWI_{fwsI}) and the right panels show the number of days per year exceeding the 95th percentile FWI (FWI_{95d}) relative to the reference period (1971-2000). **a, b)** Reference period patterns with a separate colorbar shown below, **c, d)** changes relative to the reference period at +2 °C GWL and **e, f)** changes relative to the reference period at +3 °C GWL. Note that the reference period is already 0.46 °C warmer than the preindustrial period. Areas without stippling indicate regions where at least 66% of the models project statistically significant changes according to a t-test ($p < 0.05$) and agree on the sign of change.



the local 95th percentile at lower latitudes, primarily because the fire season is longer as defined by (Wotton and Flannigan, 1993). In the Iberian Peninsula and some regions in southern Europe, there are about 18 days year⁻¹ of FWI_{95d} , indicating
 325 that the fire season defined by the temperature threshold endures almost all year.

The projected changes in FWI_{95d} relative to the reference period at 2 °C and 3 °C GWLs are shown in Figures 6d and 6f. At 2 °C, the changes are mainly confined to southern Europe, with only 25% of the total land area in the domain exhibiting robust signals (Figure 6d). In contrast, at 3 °C, significant and robust signals are projected to extend into central Europe, covering 47% of the total land area (Figure 6f). In addition, the strength of the signal becomes much more pronounced at 3 °C, with
 330 relative increases exceeding 150% in many regions, such as the Iberian Peninsula, southern France, the Balkans, and Turkey. Even regions with historically low frequencies of extreme fire weather, such as northern Europe, show increases of up to 50%. However, these increases are not statistically significant or model agreement is not established. In areas where the change signal is robust, the mean relative increase in FWI_{max} is 91% and 147%, respectively, at 2 °C and 3 °C GWLs. Overall, a general increase in the frequency of fire weather conditions is projected across Europe, with the magnitude and spatial extent
 335 of the changes becoming much more pronounced at 3 °C compared to 2 °C. However, robust changes are still mainly limited to areas south of 50° latitude even at 3 °C.

In addition to projections of the frequency of extreme fire weather, it is also important to quantify the projected changes in the magnitude of extreme fire weather. Figure 7 shows the patterns of the magnitude-based FWI metrics (left panels for FWI_{fs} and right panels for FWI_{max}) over Europe during the reference period (1971-2000) and the changes relative to the
 340 reference period at 2 °C and 3 °C GWLs based on the ensemble median of 34 bias-adjusted EURO-CORDEX models. Similar to frequency metrics, a latitudinal gradient is apparent for FWI_{fs} , with higher values concentrated mainly in southern Europe due to hot and dry summer conditions (Figure 7a). In regions such as the Iberian Peninsula, southern Italy, Greece, and Turkey FWI_{fs} values exceed 30, approaching the very high fire danger threshold of 38, as accepted by San-Miguel-Ayanz et al. (2012).

The projections show a minor relative increase in FWI_{fs} at 2 °C GWL across Europe, with the exception of regions such as Poland and northern Scandinavia (Figure 7c). However, many areas still lack robustness, with only 24% of the land area is projected to show robust signals. At +3 °C, FWI_{fs} is projected to become more widespread and intense, following the same pattern seen in frequency-based metrics (Figure 7e). It is projected to increase by more than 50% (with robust signals) not only in southern and eastern Europe, but also in regions that historically exhibited lower fire danger, such as eastern France. The
 350 percentage of land area with model agreement also increases to 43% at 3 °C. The spatially averaged relative increase in FWI_{fs} for regions with model agreement on robustness of the change signal is also projected to increase as the GWL increases: 23% at 2 °C and 44% at 3 °C.

The climatological distribution of FWI_{max} displays higher values exceeding 40 in southern Europe and lower values, usually below 20 in central to northern Europe (Figure 7b). Mountainous regions, such as the Alps and Carpathians, exhibit
 355 very low FWI_{max} values, reflecting their colder and moister climates compared to the surrounding areas. In southern Europe, regions like the Iberian Peninsula and Turkey have FWI_{max} values greater than 50, indicating that these areas experience extreme fire weather conditions annually.



The projected changes in FWI_{max} at 2 and 3 °C GWLs relative to the reference period are shown in Figures 7d and 7f, respectively. At 2 °C, the simulated positive changes are relatively small (around 10-20%). Central and northern Europe show spatial variability, including negative changes in some regions (e.g., Poland), although these are not robust signals (Figure 7d). Only 8% of the land area shows model agreement on the direction and significance of the change at 2 °C, and these areas are mostly limited to regions with very low climatological FWI_{max} values. In contrast, at 3 °C, the percentage of land area where the majority of models project robust climate change signals increases sharply to 39% (Figure 7f). However, areas with higher relative changes are still primarily the regions with low climatological values (e.g., mountainous regions), with the exception of some parts of Southern Europe, such as Italy and the Balkans, where projected increases range from 20% to 40%. Overall, in regions where change signal is robust, the simulated mean increase in FWI_{max} is 25% and 32% relative to the reference period, respectively, at 2 and 3 °C.

3.5 Sub-European Regions

In this section, we show the same fire weather metrics analyzed throughout the study (FWI_{95d} , FWI_{fws} , FWI_{max} , FWI_{fs}), but aggregate and average them over the PRUDENCE regions to highlight differences between the European sub-regions and show the spread across the model ensemble. The results are displayed as boxplots for each PRUDENCE region during the reference period (1971-2000), at 2 °C and 3 °C GWLs (Figure 8). The regions are ordered in a way that roughly corresponds to the latitude-longitude orientation (North-West to South-East) of the regions.

FWI_{95d} shows a quasi-uniform distribution across models in all PRUDENCE regions for the reference period, due to the definition of the metric and the bias adjustment of temperature, which effectively determines the start and end of the fire season based on the temperature-threshold used for overwintering DC (Figure 8a). Under both warming scenarios, the median FWI_{95d} is projected to increase across all regions with a stronger signal at 3 °C. In the Iberian Peninsula, for example, FWI_{95d} is projected to increase rapidly from a median of 16.8 days year⁻¹ during 1971-2000 to 31 days year⁻¹ at 2 °C and to 44.7 days year⁻¹ at 3 °C (Figure 8a). A similar trend is projected for France, with the median increasing from 14.5 days year⁻¹ during 1971-2000 to almost 23 days year⁻¹ at 2 °C and to 34.5 days year⁻¹ at 3 °C. In some regions, such as Eastern Europe, the model spread is large, with some models projecting a negative change, and some projecting a very extreme positive change. The model agreement is stronger in southern European regions (IP, MD, TR), where all models project a positive trend under both 2 °C and 3 °C GWLs. In addition, the spread among models increases from 2 °C to 3 °C in all regions, indicating a growing uncertainty with higher levels of warming.

There is a clear regional separation in both the reference period and projected values of FWI_{fws} , with southern European regions (IP, MD, TR) showing higher levels of fire danger than the rest of Europe (Figure 8b). However, a positive change signal is evident across almost all regions, especially at 3 °C GWL. In the Alps, a region historically characterized by shorter fire seasons, the median FWI_{fws} is projected to more than double: 14.3 days year⁻¹ during 1971-2000, to over 21 days year⁻¹ at 2 °C, and more than 31 days year⁻¹ at 3 °C. The Iberian Peninsula is projected to experience the highest absolute increase in multi-model median FWI_{fws} , rising from 43 days year⁻¹ during 1971-2000 to a projected 63 days year⁻¹ at 2 °C and almost 78 days year⁻¹ at 3 °C.

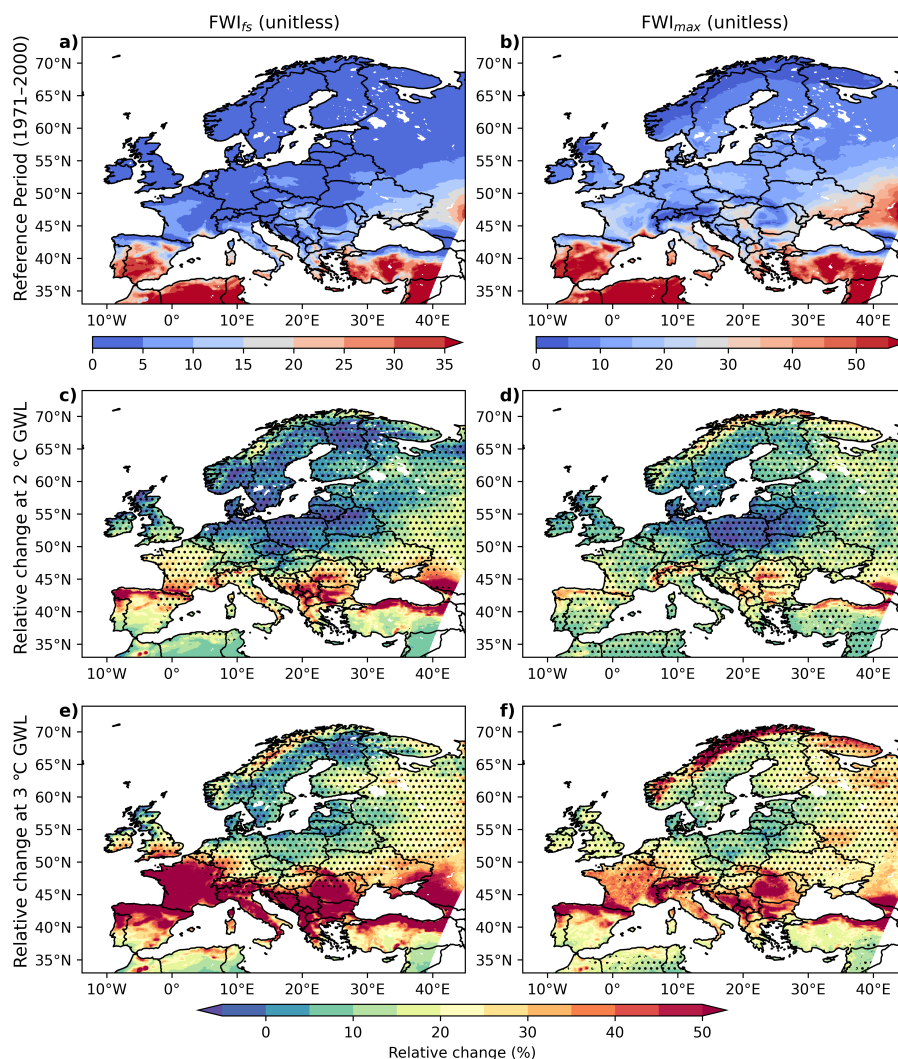


Figure 7. Patterns of magnitude-based extreme fire weather metrics and their projected changes in Europe based on the ensemble median of 34 bias-adjusted EURO-CORDEX models. The left panels show the annual peak 90-day average FWI (FWI_{fs}) and the right panels show the annual maximum FWI (FWI_{max}). **a, b** Reference period (1971-2000) patterns with a separate colorbar shown below, **c, d** changes relative to the reference period at +2 °C GWL and **e, f** changes relative to the reference period at +3 °C GWL. Note that the reference period is already 0.46 °C warmer than the preindustrial period. Areas without stippling indicate regions where at least 66% of the models project statistically significant changes according to a t-test ($p < 0.05$) and agree on the sign of change.

A clear latitudinal gradient is observed in the magnitude of FWI_{max} during the reference period and at both 2 °C and 3 °C GWLs with southern European regions exhibiting higher fire danger due to their warm and dry summer climates (Figure 8c). The main exception to this latitudinal pattern is the Alps, which exhibits lower values due to its colder and moister

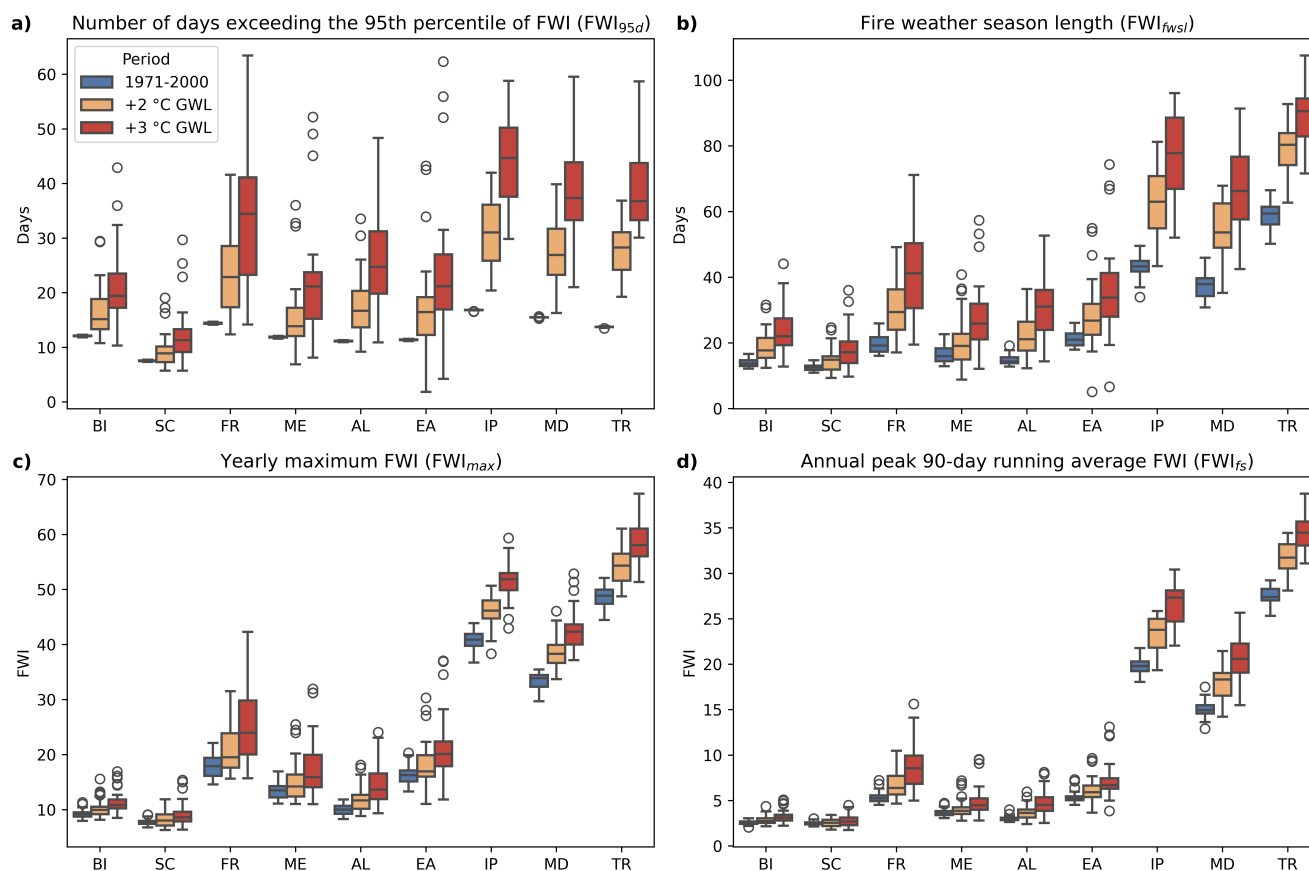


Figure 8. Model spread of FWI metrics, spatially aggregated and averaged over the PRUDENCE regions, for the reference period (blue), +2 °C GWL (orange), and +3 °C GWL (red) based on the bias-adjusted EURO-CORDEX ensemble for **a)** FWI_{95d} , **b)** FWI_{fws} , **c)** FWI_{max} , **d)** FWI_{fs} . Whiskers in the boxplots represent 1.5 times the inter-quartile range of the ensemble, with circles denoting outliers. BI = British Isles, SC = Scandinavia, FR = France, ME = Mid-Europe, AL = Alps, EA = Eastern Europe, IP = Iberian Peninsula, MD = Mediterranean, TR = Turkey.

climate conditions. Overall, the median FWI_{max} is projected to increase consistently across all regions as the GWL increases. However, the projected relative changes in FWI_{max} (Figure 8c), a magnitude-based metric, are not as pronounced as those seen in frequency-based metrics (Figures 8a and 8b). The Mediterranean, Iberian Peninsula, and Turkey clearly stand out from other regions. For instance, Turkey shows a simulated median FWI_{max} of 49 during 1971-2000, which is projected to increase to 54 at 2 °C and to 58 at 3 °C.

The FWI_{fs} (Figure 8d) is also projected to follow a similar pattern to FWI_{max} . However, the distribution ranges for FWI_{fs} are narrower than those for FWI_{max} , particularly in northern and central European regions due to the running mean. The intensity of prolonged fire weather, as represented by FWI_{fs} , is projected to increase in all regions. For example, the



median FWI_{fs} in the Mediterranean is projected to increase from 15 during 1971–2000 to 18 and 21 at 2 °C and to 3 °C GWKs, respectively.

405 In summary, all four fire weather metrics are projected to increase in all regions with increasing temperature, and more pronounced changes are expected at 3 °C GWL compared to 2 °C. In general, southern European regions (IP, MED, TR) are projected to experience more intense and prolonged extreme fire weather conditions, consistent with their baseline climatologies of dry and warm summers. Overall, the relative change signals are stronger for the frequency-based metrics (FWI_{95d} and FWI_{fws}) than for the magnitude-based metrics (FWI_{max} and FWI_{fs}). A clear latitudinal gradient is also observed, 410 with southern European regions projected to experience more severe and frequent fire weather conditions. Furthermore, the ensemble spread increases from 2 °C to 3 °C GWL, particularly for the frequency-based metrics, indicating greater uncertainty at higher warming levels.

3.6 Evaluation of Potential Drivers

Given the projected changes in extreme fire weather conditions across Europe, it is important to explain possible drivers. To 415 provide insights into this question, we examine the two main subcomponents of FWI: BUI, which represents the effects of longer-term atmospheric conditions on fuel dryness, and ISI, which reflects the influence of short-term atmospheric conditions, namely the role of wind patterns and FPMC (Ramos et al., 2023). Figure 9 illustrates FWI as a function of ISI and BUI across PRUDENCE regions, based on spatially aggregated fields from the bias-adjusted EURO-CORDEX models. The ISI–BUI pairs correspond to the averaged values for the days when FWI exceeds its 99th percentile during the reference period (1971–2000), 420 as well as at 2 °C and 3 °C GWLs for each model in the ensemble.

As global warming increases, there is a projected shift in BUI towards higher values in all regions (Figure 9). However, the signals in BI and SC are mixed, with a slight tendency towards higher fire danger (Figures 9a and 9b). In FR, ME, AL and EA regions, there is a notable shift in BUI, along with a slight increase in ISI, both of which contribute to the resulting increase FWI (Figures 9c–9f). In particular in France, the median BUI is projected to increase by almost 50% at 3 °C GWL relative to 425 the reference period, while ISI is projected to increase only by around 25%, which is an indication of the worsening of longer-term fuel drying. The increase in BUI is also apparent in the southern European regions (Figures 9g–9i). However, this does not directly translate into a significant increase in FWI in these regions because the contribution of BUI to FWI saturates at higher BUI values, consistent with the principle that there is a limit to the amount of fuel that can be used in fires (Van Wagner, 1987). Instead, in these regions, the projected increase in FWI is driven by a projected increase in ISI values, which may result from 430 an increased surface layer dryness (reflected by FPMC) or stronger winds.

To disentangle the contributions of wind speed and dryness conditions, Figure 10 shows VPD plotted against maximum wind speed across PRUDENCE regions. The VPD–wind speed pairs correspond to the averaged values for the days when FWI exceeds its 99th percentile during the reference period (1971–2000), as well as at 2 °C and 3 °C GWLs for each model in the EURO-CORDEX ensemble. The median of maximum wind speeds are projected to either decrease or remain largely 435 unchanged across all PRUDENCE regions, except in southern Europe, where a very slight increase (less than 2%) is projected, but likely not significant. In contrast, the median VPD, which reflects the thermodynamic effects of temperature and relative

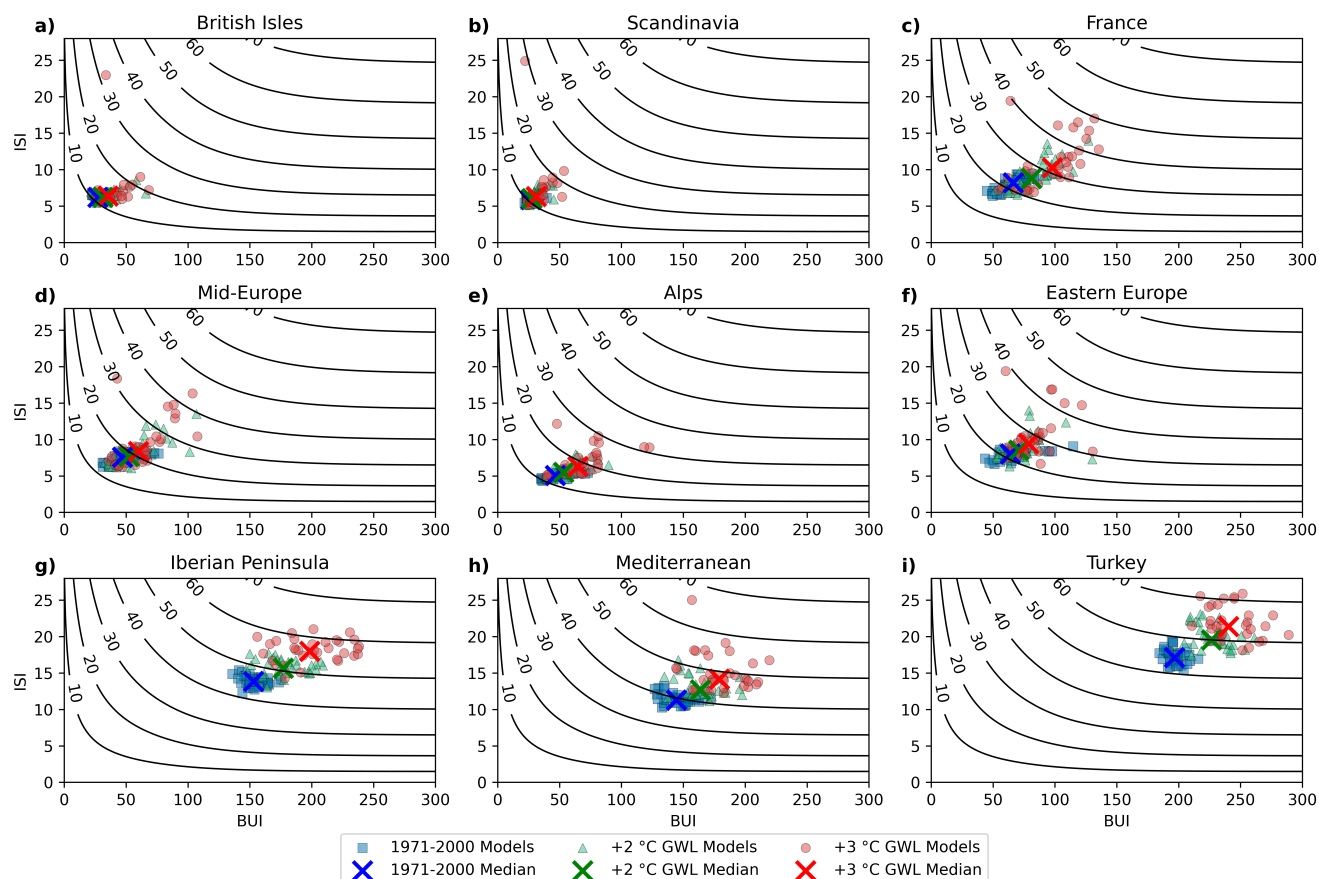


Figure 9. FWI as a function of ISI and BUI, with theoretical FWI contours overlaid for the PRUDENCE regions. ISI and BUI averages are shown for days when the FWI exceeds its 99th percentile. Blue squares denote the reference period (1971-2000), green triangles correspond to 2 °C GWL, and red circles represent 3 °C GWL. All values are spatially aggregated and area-weighted averaged over the PRUDENCE regions, namely: **a)** British Isles, **b)** Scandinavia, **c)** France, **d)** Mid-Europe, **e)** Alps, **f)** Eastern Europe, **g)** Iberian Peninsula, **h)** Mediterranean, and **i)** Turkey. Each value corresponds to a bias adjusted EURO-CORDEX model; crosses indicate ensemble medians.

humidity through atmospheric drying, is projected to increase across all regions, with particularly strong increases in central and southern Europe. In southern European regions, the projected increase in the median VPD on days when FWI exceeds its 99th percentile at 3 °C GWL relative to the reference period is almost 40%, with some models projecting changes larger than 70% (Figures 10g-10i). This suggests that the projected changes in FWI are primarily driven by increased fuel aridity due to thermodynamic drivers rather than dynamical drivers through the changes in wind speeds. This may also indicate that the projected changes in ISI in southern Europe (Figure 9) are largely influenced by increased surface layer fuel dryness (FFMC), rather than wind speed.

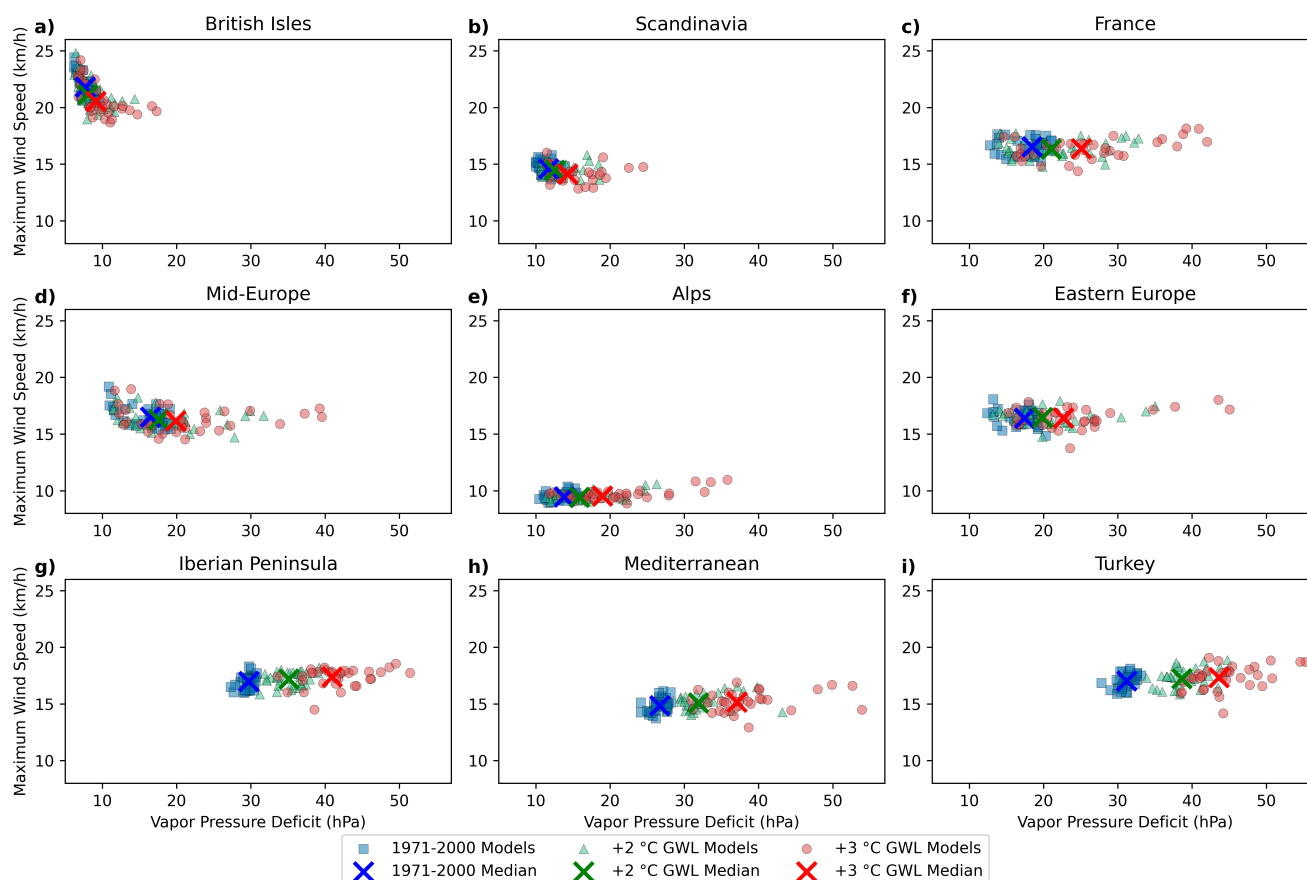


Figure 10. VPD (hPa) vs. maximum wind speed (km/h) for the PRUDENCE regions. VPD and maximum wind speed averages are shown for days when the FWI exceeds its 99th percentile. Blue squares denote the reference period (1971–2000), green triangles correspond to 2 °C GWL, and red circles represent 3 °C GWL. All values are spatially aggregated and area-weighted averaged over the PRUDENCE regions, namely **a)** British Isles, **b)** Scandinavia, **c)** France, **d)** Mid-Europe, **e)** Alps, **f)** Eastern Europe, **g)** Iberian Peninsula, **h)** Mediterranean, and **i)** Turkey. Each value corresponds to a bias adjusted EURO-CORDEX model; crosses indicate ensemble medians. Note that the VPD values are likely overestimated, as they are calculated using maximum temperature and relative humidity.



4 Summary and Discussion

445 This study assesses how extreme fire weather in Europe is influenced by recent and future climate change. With this aim, it also evaluates the performance of EURO-CORDEX simulations in representing the extreme fire weather and the potential improvements offered by bias adjustment with QDM. The main results are as follows:

1. The most suitable combination of daily input variables to approximate typical noon-time FWI includes maximum temperature, accumulated precipitation, mean relative humidity, and maximum wind speed. These atmospheric fields were
 450 selected on the basis of their relatively lower bias in the resulting FWI calculations and broader model availability in the EURO-CORDEX ensemble.
2. An analysis of the historical period (1950–2023) based on ERA5-Land reanalysis data revealed a clear latitudinal gradient in extreme fire weather, with more severe conditions occurring in southern Europe. A positive trend in the frequency and magnitude of extreme fire weather has been observed since the 1950s across many regions, such that 29% and 37%
 455 of the land area exhibited a significant trend in FWI_{mid} and FWI_{95d} , respectively. The majority of the significant trends for both metrics were concentrated in the Iberian Peninsula, Central Europe, and Ukraine, with positive trends nearly everywhere.
3. As the raw model outputs from the EURO-CORDEX framework have systematic biases (Vautard et al., 2021), the input fields were bias adjusted before calculating the FWI. The bias adjustment of the input fields with QDM significantly
 460 reduced the resulting FWI bias during the calibration period. Bias relative to the ERA5-Land for the 95th percentile of FWI in the EURO-CORDEX ensemble median is reduced from 78% to below 9%.
4. EURO-CORDEX future projections show that extreme fire weather in Europe is projected to become more widespread, more frequent, and more intense with increasing GWL, consistent with previous assessments (Abatzoglou et al., 2019; El Garroussi et al., 2024; Hetzer et al., 2024; Jones et al., 2022). Relative increases in frequency-based extreme fire
 465 weather metrics are larger than those for magnitude-based metrics. The spatial extent of robust signals is projected to nearly double at 3 °C GWL compared to 2 °C for three of the four metrics. For FWI_{max} , the spatial extent at 3 °C is almost five times that of at 2 °C.
5. A latitudinal gradient is also evident in the projected fire weather danger, where southern European regions (the Iberian Peninsula, the Mediterranean and Turkey) are expected to experience longer and more intense fire weather conditions.
 470 The frequency and magnitude of extreme fire weather are also projected to increase in regions such as France, the Alps, Eastern Europe, and Mid-Europe, particularly at 3 °C GWL.
6. The subcomponents of the FWI system, namely the BUI and the ISI are projected to increase in most regions, although with a relatively smaller increase for ISI. In regions such as France and Eastern Europe, contribution to the increase in FWI is shared between BUI and ISI. However, since the influence of BUI on FWI saturates beyond a certain threshold



(Van Wagner, 1987) and southern European regions already exhibit very high BUI values, changes in ISI emerge as the dominant driver of the increase in FWI in these regions.

7. The relevance of projected changes in wind speed are marginal, whereas the VPD is projected to increase across all regions. This indicates that thermodynamic factors are the primary contributors to the projected changes in extreme fire weather in Europe. This finding aligns with a growing body of evidence indicating that increased fuel dryness is the key driver behind both observed and projected increases in fire weather in many regions worldwide (Clarke et al., 2022; Ellis et al., 2022; Jain et al., 2022; Resco de Dios et al., 2021; Williams et al., 2019).

The evaluation period used for the bias adjustment performance assessment was the same period used for the calibration (1971–2000), as it was important to utilize a longer period to reduce sampling uncertainty, and the historical time series from the EURO-CORDEX simulations are not long enough to allocate a separate validation period. Since uncertainty may arise from the choice of bias correction methods, some studies have shown that the application of a multivariate bias adjustment method that not only adjusts the marginal distributions but also inter-variable dependencies can further improve the model performance in representing the multivariate hazard estimates (Cannon, 2018; Zscheischler et al., 2019). However, they usually come with greater computational cost (e.g., Cannon (2018)). We suggest that there is still a need for further research on the performance of univariate and multivariate bias adjustment methods for the multivariate hazard estimates at a pan-European scale with a relatively large model ensemble.

Although extreme fire weather conditions, as represented by the FWI, are projected to intensify in terms of both frequency and magnitude, it is important to emphasize that the FWI is a fire weather rating metric and not a measure of fire occurrence. In fact, fire weather creates conditions that may enhance the susceptibility of landscapes to other key wildfire drivers, namely ignition, fuel dryness and fuel continuity (Pausas and Keeley, 2021). It remains unclear whether these bioclimatic and anthropogenic factors will remain unchanged in Europe in the future. In general, FWI provides the most meaningful danger information in regions where fire activity is limited by fuel dryness rather than by vegetation productivity (Jones et al., 2022). Nevertheless, the strongest relationships between FWI and burned area are observed in ecosystems with intermediate moisture availability (Jones et al., 2022), including boreal and evergreen forests (Abatzoglou et al., 2018; Bedia et al., 2015), as well as in Mediterranean Europe (Carvalho et al., 2008; Calheiros et al., 2020; Fox et al., 2018; Jones et al., 2022; Urbieto et al., 2015). Furthermore, since the relationship between FWI and fire occurrence — and the thresholds for what constitutes extreme — varies regionally, it is important to incorporate regional climate and biome characteristics when interpreting FWI values for fire danger assessments to improve early warning systems and fire mitigation strategies in a changing climate (Kudláčková et al., 2024).

The ecosystem and socioeconomic impacts of a fire depend not only on fire weather, the availability of flammable vegetation, and ignition sources, but also on forest management practices prior to fire events and suppression efforts. For instance, the burned area in the Mediterranean has shown a declining trend since the 1980s, primarily due to enhanced suppression strategies (Turco et al., 2016), despite increasing trends in fire weather. However, the increasing pressure from climate change and more extreme fire weather may lead to conditions where high-intensity fires overwhelm the suppression capacity (Abatzoglou et al.,



2021; Podur and Wotton, 2010). In response to this growing challenge, international resource sharing has been recognized
 510 as both necessary and effective in Europe (Bloem et al., 2022) and RescEU has been established as a collective response of
 European member states to this growing need by pooling resources (Hopkins and Faulkner, 2021). However, it is also critical
 to recognize the so-called "fire-fighting trap" or the "suppression paradox", where extinguishing all fires at any cost may lead
 to fires with greater severity in the following years under extreme fire weather conditions, due to fuel accumulation over time
 (Kreider et al., 2024; Moreira et al., 2020; Parisien et al., 2020). Given that the duration and intensity of extreme fire weather
 515 conditions are projected to increase with increasing greenhouse gas emissions, particularly in Mediterranean-type climates, a
 paradigm shift is advocated, emphasizing the importance of mitigation measures (Moreira et al., 2020). In this context, policy
 effectiveness should not be measured solely by the extent of the burned area, but rather by the degree to which socio-ecological
 damage is avoided (Moreira et al., 2020).

The next generation of simulations in the EURO-CORDEX framework, downscaled from CMIP6 GCMs, is currently un-
 520 derway (Katrakou et al., 2024), with some outputs expected to become available soon. This new generation of simulations
 retains the same spatial resolution as their CMIP5 counterparts, but incorporates greenhouse gas forcing scenarios based on
 the state-of-the-art Shared Socioeconomic Pathways (SSPs) instead of RCPs, along with a consistent space- and time-varying
 aerosol forcing (Katrakou et al., 2024). The latter may lead to a better representation of regional extreme fire weather con-
 ditions, considering that models that do not account for time-evolving aerosols underestimate the European summer warming
 525 (Schumacher et al., 2024). In this sense, FWI-based analyses can serve as a useful framework to evaluate whether newer model
 generations improve the representation of complex, multivariate weather hazards. Future studies should also employ these
 RCMs for further investigation while accounting for the "hot model problem" that was identified shortly after the release of
 the associated GCMs (Hausfather et al., 2022). The present study can thus be seen as one more piece of the puzzle towards
 advancing our understanding of extreme fire weather in Europe in a warming climate, while emphasizing the need for measures
 530 to protect vulnerable regions.

Code and data availability. The QDM implementation is based on the Python package cmethods (Schwertfeger et al., 2023), available at
<https://python-cmethods.readthedocs.io/en/latest/>. Singularity Stochastic Removal, seasonal cycle correction, and relative change signal ad-
 justment were implemented on top of this package by the authors of this study. FWI calculations were performed using a Python script
 provided by Quilcaille et al. (2023) and available at https://github.com/yquilcaille/FWI_CMIP6. All datasets used in this study are publicly
 535 available. ERA5-Land hourly reanalysis data are available at <https://cds.climate.copernicus.eu/datasets/reanalysis-era5-land>. CMIP5 global
 climate model and EURO-CORDEX regional climate model data are available from the Earth System Grid Federation node at the Ger-
 man Climate Computing Center through <https://esgf-metagrid.cloud.dkrz.de/search?project=CMIP5> and <https://esgf-metagrid.cloud.dkrz.de/search?project=CORDEX>.



Appendix A: Further Details on Bias Adjustment of EURO-CORDEX Model Outputs

540 Various methods have been developed for bias adjustment (Maraun, 2016), among which quantile-based univariate methods are arguably one of the most widely used. For this study, we selected the Quantile Delta Mapping (QDM) method (Cannon et al., 2015) to adjust the biases in the input fields from EURO-CORDEX simulations, which were then used to calculate the FWI. QDM is selected due to its ability to adjust biases in each quantile while preserving the relative change signal of the underlying climate model, as demonstrated for precipitation- and temperature-based indices (Cannon et al., 2015; Casanueva
545 et al., 2020; Tong et al., 2021; Xavier et al., 2022). The fundamental QDM calculation procedure is given in the main text (see Section 2.2.1) with further details provided below.

Quantile-based methods can inherently correct the so-called drizzle effect, where models simulate too many rainy days compared to the reference data (Argüeso et al., 2013; Gutowski et al., 2003; Van de Velde et al., 2021), by multiplying the lower end of the distribution by zero. To address cases where modeled dry days are more frequent than in the reference data,
550 Cannon et al. (2015) replaced dry days in both modeled and observed data with uniformly distributed non-zero values below a specified threshold prior to bias adjustment. After the bias adjustment, values below the threshold are returned to zero. This approach has later been referred to as Singularity Stochastic Removal (SSR) (Lehner et al., 2023; Vrac et al., 2016). SSR was applied here using a threshold of 0.05 mm day^{-1} to adjust occurrence biases in the EURO-CORDEX precipitation simulations, and a more conservative threshold of 0.1 mm day^{-1} was used to reset the values to zero after bias adjustment.

555 The biases in the seasonal cycle of each atmospheric field were adjusted using a three-month running window centered on the month of interest (Cannon et al., 2015). Future simulation periods were adjusted in separate 10-year batches to preserve climate change signals and reduce computational demands.



Appendix B: Global Warming Levels based on CMIP5 Simulations

Table B1. Thirty-year time periods when the specified global warming level relative to the preindustrial period is reached for the first time by the GCMs used as boundary conditions for the RCMs used in this study (scenario: RCP8.5). Note that each model follows a different trajectory to reach the relevant GWLs due to differences in climate sensitivity. For all simulations, preindustrial baseline period is 1881-1910, which is 0.46 °C colder than the reference period (1971-2000).

GCM	+2 °C GWL Period	+3 °C GWL Period
CNRM-CERFACS-CNRM-CM5	2029-2058	2052-2081
ICHEC-EC-EARTH	2028-2057	2052-2081
IPSL-IPSL-CM5A-MR	2020-2049	2039-2068
MOHC-HadGEM2-ES	2016-2045	2037-2066
MPI-M-MPI-ESM-LR	2029-2058	2052-2081
NCC-NorESM1-M	2031-2060	2057-2086

Appendix C: FWI Proxy Input Combinatinations

Table C1. FWI input combinations tested in this study to approximate the original noon-time FWI calculation.

Combination	Temperature	Precipitation	Relative Humidity	Wind Speed
Original	at noon	accumulated at noon	at noon	at noon
Comb-1	daily maximum	accumulated daily	daily mean	daily maximum
Comb-2	daily maximum	accumulated daily	daily mean	daily mean
Comb-3	daily maximum	accumulated daily	daily minimum	daily maximum
Comb-4	daily maximum	accumulated daily	daily minimum	daily mean



560 *Author contributions.* ASB: conceptualization, data curation, formal analysis, methodology, software, visualization, writing - original draft.
JGP: conceptualization, methodology, resources, supervision, writing - review & editing. CMG: conceptualization, methodology, writing -
review & editing. AMR: conceptualization, methodology, project administration, resources, supervision, writing - review & editing.

Competing interests. The authors declare that they have no conflict of interest.

Acknowledgements. We acknowledge support by the KIT-Publication Fund of the Karlsruhe Institute of Technology. The authors thank
565 the German Climate Computing Center (DKRZ) for providing the computing resources. We also acknowledge the World Climate Re-
search Program's Working Group on Coupled Modeling, which is responsible for CMIP, and the relevant climate modeling groups (listed
in Table 1) for producing and making the CMIP5 output available. We also acknowledge the CORDEX community for producing the
EURO-CORDEX simulations and making them available (listed in Table 1). AI-assisted tools (ChatGPT, OpenAI) were used for minor
language editing of this manuscript. AMR was supported by the Helmholtz "Changing Earth - Sustaining our Future" program. JGP thanks
570 the AXA Research Fund for support. The contribution of CMG was performed under the framework of the DHEFEUS project, funded
by FCT (<https://doi.org/10.54499/2022.09185.PTDC>). The authors thank Hendrik Feldmann and Florian Ehmele (both IMKTRO, KIT) for
discussions on EURO-CORDEX models and bias adjustment.



References

- Abatzoglou, J. T. and Williams, A. P.: Impact of anthropogenic climate change on wildfire across western US forests, *Proceedings of the National Academy of Sciences*, 113, 11 770–11 775, <https://doi.org/10.1073/pnas.1607171113>, 2016.
- Abatzoglou, J. T., Williams, A. P., Boschetti, L., Zubkova, M., and Kolden, C. A.: Global patterns of interannual climate–fire relationships, *Global Change Biology*, 24, 5164–5175, <https://doi.org/10.1111/gcb.14405>, 2018.
- Abatzoglou, J. T., Williams, A. P., and Barbero, R.: Global Emergence of Anthropogenic Climate Change in Fire Weather Indices, *Geophysical Research Letters*, 46, 326–336, <https://doi.org/10.1029/2018GL080959>, 2019.
- Abatzoglou, J. T., Juang, C. S., Williams, A. P., Kolden, C. A., and Westerling, A. L.: Increasing Synchronous Fire Danger in Forests of the Western United States, *Geophysical Research Letters*, 48, e2020GL091 377, <https://doi.org/10.1029/2020GL091377>, 2021.
- Alduchov, O. A. and Eskridge, R. E.: Improved Magnus Form Approximation of Saturation Vapor Pressure, *Journal of Applied Meteorology and Climatology*, 35, 601–609, [https://doi.org/10.1175/1520-0450\(1996\)035<0601:IMFAOS>2.0.CO;2](https://doi.org/10.1175/1520-0450(1996)035<0601:IMFAOS>2.0.CO;2), 1996.
- Andela, N., Morton, D. C., Giglio, L., Chen, Y., van der Werf, G. R., Kasibhatla, P. S., DeFries, R. S., Collatz, G. J., Hantson, S., Kloster, S., Bachelet, D., Forrest, M., Lasslop, G., Li, F., Mangeon, S., Melton, J. R., Yue, C., and Randerson, J. T.: A human-driven decline in global burned area, *Science*, 356, 1356–1362, <https://doi.org/10.1126/science.aal4108>, 2017.
- Argüeso, D., Evans, J. P., and Fita, L.: Precipitation bias correction of very high resolution regional climate models, *Hydrology and Earth System Sciences*, 17, 4379–4388, <https://doi.org/10.5194/hess-17-4379-2013>, 2013.
- Bayar, A. S., Yılmaz, M. T., Yücel, I., and Dirmeyer, P.: CMIP6 Earth System Models Project Greater Acceleration of Climate Zone Change Due To Stronger Warming Rates, *Earth’s Future*, 11, e2022EF002 972, <https://doi.org/10.1029/2022EF002972>, 2023.
- Bedia, J., Herrera, S., Gutiérrez, J. M., Benali, A., Brands, S., Mota, B., and Moreno, J. M.: Global patterns in the sensitivity of burned area to fire-weather: Implications for climate change, *Agricultural and Forest Meteorology*, 214–215, 369–379, <https://doi.org/10.1016/j.agrformet.2015.09.002>, 2015.
- Bento, V. A., Lima, D. C. A., Santos, L. C., Lima, M. M., Russo, A., Nunes, S. A., DaCamara, C. C., Trigo, R. M., and Soares, P. M. M.: The future of extreme meteorological fire danger under climate change scenarios for Iberia, *Weather and Climate Extremes*, 42, 100 623, <https://doi.org/10.1016/j.wace.2023.100623>, 2023.
- Bentsen, M., Bethke, I., Debernard, J. B., Iversen, T., Kirkevåg, A., Seland, , Drange, H., Roelandt, C., Seierstad, I. A., Hoose, C., and Kristjánsson, J. E.: The Norwegian Earth System Model, NorESM1-M – Part 1: Description and basic evaluation of the physical climate, *Geoscientific Model Development*, 6, 687–720, <https://doi.org/10.5194/gmd-6-687-2013>, 2013.
- Bloem, S., Cullen, A. C., Mearns, L. O., and Abatzoglou, J. T.: The Role of International Resource Sharing Arrangements in Managing Fire in the Face of Climate Change, *Fire*, 5, 88, <https://doi.org/10.3390/fire5040088>, 2022.
- Bowman, D. M. J. S., Balch, J. K., Artaxo, P., Bond, W. J., Carlson, J. M., Cochrane, M. A., D’Antonio, C. M., DeFries, R. S., Doyle, J. C., Harrison, S. P., Johnston, F. H., Keeley, J. E., Krawchuk, M. A., Kull, C. A., Marston, J. B., Moritz, M. A., Prentice, I. C., Roos, C. I., Scott, A. C., Swetnam, T. W., Werf, G. R. v. d., and Pyne, S. J.: Fire in the Earth System, *Science*, 324, 481–484, <https://doi.org/10.1126/science.1163886>, 2009.
- Bowman, D. M. J. S., Williamson, G. J., Abatzoglou, J. T., Kolden, C. A., Cochrane, M. A., and Smith, A. M. S.: Human exposure and sensitivity to globally extreme wildfire events, *Nature Ecology & Evolution*, 1, 1–6, <https://doi.org/10.1038/s41559-016-0058>, 2017.
- Bowman, D. M. J. S., Kolden, C. A., Abatzoglou, J. T., Johnston, F. H., van der Werf, G. R., and Flannigan, M.: Vegetation fires in the Anthropocene, *Nature Reviews Earth & Environment*, 1, 500–515, <https://doi.org/10.1038/s43017-020-0085-3>, 2020.



- 610 Bøssing Christensen, O., Drews, M., Hesselbjerg Christensen, J., Dethloff, K., Ketelsen, K., Hebestadt, I., and Rinke, A.: The HIRHAM Regional Climate Model. Version 5 (beta), Technical Report 06-17, Danish Climate Centre, Danish Meteorological Institute, 2007.
- Calheiros, T., Nunes, J. P., and Pereira, M. G.: Recent evolution of spatial and temporal patterns of burnt areas and fire weather risk in the Iberian Peninsula, *Agricultural and Forest Meteorology*, 287, 107923, <https://doi.org/10.1016/j.agrformet.2020.107923>, 2020.
- Calheiros, T., Pereira, M. G., and Nunes, J. P.: Assessing impacts of future climate change on extreme fire weather and pyro-regions in Iberian Peninsula, *Science of The Total Environment*, 754, 142233, <https://doi.org/10.1016/j.scitotenv.2020.142233>, 2021.
- 615 Cannon, A. J.: Multivariate quantile mapping bias correction: an N-dimensional probability density function transform for climate model simulations of multiple variables, *Climate Dynamics*, 50, 31–49, <https://doi.org/10.1007/s00382-017-3580-6>, 2018.
- Cannon, A. J., Sobie, S. R., and Murdock, T. Q.: Bias Correction of GCM Precipitation by Quantile Mapping: How Well Do Methods Preserve Changes in Quantiles and Extremes?, *Journal of Climate*, 28, 6938–6959, <https://doi.org/10.1175/JCLI-D-14-00754.1>, 2015.
- 620 Carnicer, J., Alegria, A., Giannakopoulos, C., Di Giuseppe, F., Karali, A., Koutsias, N., Lionello, P., Parrington, M., and Vitolo, C.: Global warming is shifting the relationships between fire weather and realized fire-induced CO₂ emissions in Europe, *Scientific Reports*, 12, 10365, <https://doi.org/10.1038/s41598-022-14480-8>, 2022.
- Carvalho, A., Flannigan, M. D., Logan, K., Miranda, A. I., and Borrego, C.: Fire activity in Portugal and its relationship to weather and the Canadian Fire Weather Index System, *International Journal of Wildland Fire*, 17, 328–338, <https://doi.org/10.1071/WF07014>, 2008.
- 625 Casanueva, A., Herrera, S., Iturbide, M., Lange, S., Jury, M., Dosio, A., Maraun, D., and Gutiérrez, J. M.: Testing bias adjustment methods for regional climate change applications under observational uncertainty and resolution mismatch, *Atmospheric Science Letters*, 21, e978, <https://doi.org/10.1002/asl.978>, 2020.
- Chen, J., Arsenault, R., Brissette, F. P., and Zhang, S.: Climate Change Impact Studies: Should We Bias Correct Climate Model Outputs or Post-Process Impact Model Outputs?, *Water Resources Research*, 57, e2020WR028638, <https://doi.org/10.1029/2020WR028638>, 2021.
- 630 Christensen, J. H. and Christensen, O. B.: A summary of the PRUDENCE model projections of changes in European climate by the end of this century, *Climatic Change*, 81, 7–30, <https://doi.org/10.1007/s10584-006-9210-7>, 2007.
- Chuvieco, E., Lizundia-Loiola, J., Pettinari, M. L., Ramo, R., Padilla, M., Tansey, K., Mouillot, F., Laurent, P., Storm, T., Heil, A., and Plummer, S.: Generation and analysis of a new global burned area product based on MODIS 250m reflectance bands and thermal anomalies, *Earth System Science Data*, 10, 2015–2031, <https://doi.org/10.5194/essd-10-2015-2018>, 2018.
- 635 Clarke, H., Nolan, R. H., De Dios, V. R., Bradstock, R., Griebel, A., Khanal, S., and Boer, M. M.: Forest fire threatens global carbon sinks and population centres under rising atmospheric water demand, *Nature Communications*, 13, 7161, <https://doi.org/10.1038/s41467-022-34966-3>, 2022.
- Collins, W. J., Bellouin, N., Doutriaux-Boucher, M., Gedney, N., Halloran, P., Hinton, T., Hughes, J., Jones, C. D., Joshi, M., Liddicoat, S., Martin, G., O'Connor, F., Rae, J., Senior, C., Sitch, S., Totterdell, I., Wiltshire, A., and Woodward, S.: Development and evaluation of an Earth-System model – HadGEM2, *Geoscientific Model Development*, 4, 1051–1075, <https://doi.org/10.5194/gmd-4-1051-2011>, 2011.
- 640 Copernicus Climate Change Service (C3S) and (WMO), W. M. O.: European State of the Climate 2024, Tech. rep., Copernicus Climate Change Service (C3S), <https://climate.copernicus.eu/esotc/2024>, 2025.
- Cunningham, C. X., Williamson, G. J., and Bowman, D. M. J. S.: Increasing frequency and intensity of the most extreme wildfires on Earth, *Nature Ecology & Evolution*, 8, 1420–1425, <https://doi.org/10.1038/s41559-024-02452-2>, 2024.
- 645 de Rigo, D., Libertà, G., Houston Durrant, T., Vivancos, T. A., San-Miguel-Ayán, J., and Union, P. O. o. t. E.: Forest fire danger extremes in Europe under climate change: variability and uncertainty, Research Report, Publications Office of the European Union, 2017.



- Dosio, A. and Paruolo, P.: Bias correction of the ENSEMBLES high-resolution climate change projections for use by impact models: Evaluation on the present climate, *Journal of Geophysical Research: Atmospheres*, 116, <https://doi.org/10.1029/2011JD015934>, 2011.
- Dufresne, J.-L., Foujols, M.-A., Denvil, S., Caubel, A., Marti, O., Aumont, O., Balkanski, Y., Bekki, S., Bellenger, H., Benshila, R., Bony, S., Bopp, L., Braconnot, P., Brockmann, P., Cadule, P., Cheruy, F., Codron, F., Cozic, A., Cugnet, D., de Noblet, N., Duvel, J.-P., Ethé, C., Fairhead, L., Fichet, T., Flavoni, S., Friedlingstein, P., Grandpeix, J.-Y., Guez, L., Guilyardi, E., Hauglustaine, D., Hourdin, F., Idelkadi, A., Ghattas, J., Joussaume, S., Kageyama, M., Krinner, G., Labetoulle, S., Lahellec, A., Lefebvre, M.-P., Lefevre, F., Levy, C., Li, Z. X., Lloyd, J., Lott, F., Madec, G., Mancip, M., Marchand, M., Masson, S., Meurdesoif, Y., Mignot, J., Musat, I., Parouty, S., Polcher, J., Rio, C., Schulz, M., Swingedouw, D., Szopa, S., Talandier, C., Terray, P., Viovy, N., and Vuichard, N.: Climate change projections using the IPSL-CM5 Earth System Model: from CMIP3 to CMIP5, *Climate Dynamics*, 40, 2123–2165, <https://doi.org/10.1007/s00382-012-1636-1>, 2013.
- El Garroussi, S., Di Giuseppe, F., Barnard, C., and Wetterhall, F.: Europe faces up to tenfold increase in extreme fires in a warming climate, *npj Climate and Atmospheric Science*, 7, 30, <https://doi.org/10.1038/s41612-024-00575-8>, 2024.
- Ellis, T. M., Bowman, D. M. J. S., Jain, P., Flannigan, M. D., and Williamson, G. J.: Global increase in wildfire risk due to climate-driven declines in fuel moisture, *Global Change Biology*, 28, 1544–1559, <https://doi.org/10.1111/gcb.16006>, 2022.
- Eyring, V., Bony, S., Meehl, G. A., Senior, C. A., Stevens, B., Stouffer, R. J., and Taylor, K. E.: Overview of the Coupled Model Intercomparison Project Phase 6 (CMIP6) experimental design and organization, *Geoscientific Model Development*, 9, 1937–1958, <https://doi.org/10.5194/gmd-9-1937-2016>, 2016.
- Fargeon, H., Pimont, F., Martin-StPaul, N., De Caceres, M., Ruffault, J., Barbero, R., and Dupuy, J.-L.: Projections of fire danger under climate change over France: where do the greatest uncertainties lie?, *Climatic Change*, 160, 479–493, <https://doi.org/10.1007/s10584-019-02629-w>, 2020.
- Fox, D. M., Carrega, P., Ren, Y., Caillouet, P., Bouillon, C., and Robert, S.: How wildfire risk is related to urban planning and Fire Weather Index in SE France (1990–2013), *Science of The Total Environment*, 621, 120–129, <https://doi.org/10.1016/j.scitotenv.2017.11.174>, 2018.
- Friedlingstein, P., O’Sullivan, M., Jones, M. W., Andrew, R. M., Hauck, J., Landschützer, P., Le Quéré, C., Li, H., Luijckx, I. T., Olsen, A., Peters, G. P., Peters, W., Pongratz, J., Schwingshackl, C., Sitch, S., Canadell, J. G., Ciais, P., Jackson, R. B., Alin, S. R., Arneeth, A., Arora, V., Bates, N. R., Becker, M., Bellouin, N., Berghoff, C. F., Bittig, H. C., Bopp, L., Cadule, P., Campbell, K., Chamberlain, M. A., Chandra, N., Chevallier, F., Chini, L. P., Colligan, T., Decayeux, J., Djeutchouang, L. M., Dou, X., Duran Rojas, C., Enyo, K., Evans, W., Fay, A. R., Feely, R. A., Ford, D. J., Foster, A., Gasser, T., Gehlen, M., Gkritzalis, T., Grassi, G., Gregor, L., Gruber, N., Gürses, , Harris, I., Hefner, M., Heinke, J., Hurtt, G. C., Iida, Y., Ilyina, T., Jacobson, A. R., Jain, A. K., Jarníková, T., Jersild, A., Jiang, F., Jin, Z., Kato, E., Keeling, R. F., Klein Goldewijk, K., Knauer, J., Korsbakken, J. I., Lan, X., Lauvset, S. K., Lefèvre, N., Liu, Z., Liu, J., Ma, L., Maksyutov, S., Marland, G., Mayot, N., McGuire, P. C., Metzl, N., Monacchi, N. M., Morgan, E. J., Nakaoka, S.-I., Neill, C., Niwa, Y., Nützel, T., Olivier, L., Ono, T., Palmer, P. I., Pierrot, D., Qin, Z., Resplandy, L., Roobaert, A., Rosan, T. M., Rödenbeck, C., Schwinger, J., Smallman, T. L., Smith, S. M., Sospedra-Alfonso, R., Steinhoff, T., Sun, Q., Sutton, A. J., Séférián, R., Takao, S., Tatebe, H., Tian, H., Tilbrook, B., Torres, O., Tourigny, E., Tsujino, H., Tubiello, F., van der Werf, G., Wanninkhof, R., Wang, X., Yang, D., Yang, X., Yu, Z., Yuan, W., Yue, X., Zaehle, S., Zeng, N., and Zeng, J.: Global Carbon Budget 2024, *Earth System Science Data*, 17, 965–1039, <https://doi.org/10.5194/essd-17-965-2025>, 2025.
- Galizia, L. F., Barbero, R., Rodrigues, M., Ruffault, J., Pimont, F., and Curt, T.: Global Warming Reshapes European Pyroregions, *Earth’s Future*, 11, e2022EF003182, <https://doi.org/10.1029/2022EF003182>, 2023.



- Giorgetta, M. A., Jungclaus, J., Reick, C. H., Legutke, S., Bader, J., Böttinger, M., Brovkin, V., Crueger, T., Esch, M., Fieg, K., Glushak, K., Gayler, V., Haak, H., Hollweg, H.-D., Ilyina, T., Kinne, S., Kornblueh, L., Matei, D., Mauritsen, T., Mikolajewicz, U., Mueller, W., Notz, D., Pithan, F., Raddatz, T., Rast, S., Redler, R., Roeckner, E., Schmidt, H., Schnur, R., Segschneider, J., Six, K. D., Stockhause, M., Timmreck, C., Wegner, J., Widmann, H., Wieners, K.-H., Claussen, M., Marotzke, J., and Stevens, B.: Climate and carbon cycle changes from 1850 to 2100 in MPI-ESM simulations for the Coupled Model Intercomparison Project phase 5, *Journal of Advances in Modeling Earth Systems*, 5, 572–597, <https://doi.org/10.1002/jame.20038>, 2013.
- Giorgi, F.: Thirty Years of Regional Climate Modeling: Where Are We and Where Are We Going next?, *Journal of Geophysical Research: Atmospheres*, 124, 5696–5723, <https://doi.org/10.1029/2018JD030094>, 2019.
- Gumus, B., Oruc, S., Yucel, I., and Yilmaz, M. T.: Impacts of Climate Change on Extreme Climate Indices in Türkiye Driven by High-Resolution Downscaled CMIP6 Climate Models, *Sustainability*, 15, 7202, <https://doi.org/10.3390/su15097202>, 2023.
- Gutowski, W. J., Decker, S. G., Donavon, R. A., Pan, Z., Arritt, R. W., and Takle, E. S.: Temporal–Spatial Scales of Observed and Simulated Precipitation in Central U.S. Climate, *Journal of Climate*, 16, 3841–3847, [https://doi.org/10.1175/1520-0442\(2003\)016<3841:TSSOAS>2.0.CO;2](https://doi.org/10.1175/1520-0442(2003)016<3841:TSSOAS>2.0.CO;2), 2003.
- Hakala, K., Addor, N., and Seibert, J.: Hydrological Modeling to Evaluate Climate Model Simulations and Their Bias Correction, *Journal of Hydrometeorology*, 19, <https://doi.org/10.1175/JHM-D-17-0189.1>, section: *Journal of Hydrometeorology*, 2018.
- Hausfather, Z., Marvel, K., Schmidt, G. A., Nielsen-Gammon, J. W., and Zelinka, M.: Climate simulations: recognize the ‘hot model’ problem, *Nature*, 605, 26–29, <https://doi.org/10.1038/d41586-022-01192-2>, 2022.
- Hazeleger, W., Wang, X., Severijns, C., Ștefănescu, S., Bintanja, R., Sterl, A., Wyser, K., Semmler, T., Yang, S., van den Hurk, B., van Noije, T., van der Linden, E., and van der Wiel, K.: EC-Earth V2.2: description and validation of a new seamless earth system prediction model, *Climate Dynamics*, 39, 2611–2629, <https://doi.org/10.1007/s00382-011-1228-5>, 2012.
- He, Q., Williams, A. P., Johnston, M. R., Juang, C. S., and Wang, B.: Influence of Time-Averaging of Climate Data on Estimates of Atmospheric Vapor Pressure Deficit and Inferred Relationships With Wildfire Area in the Western United States, *Geophysical Research Letters*, 52, e2024GL113708, <https://doi.org/10.1029/2024GL113708>, 2025.
- He, T., Lamont, B. B., and Pausas, J. G.: Fire as a key driver of Earth’s biodiversity, *Biological Reviews*, 94, 1983–2010, <https://doi.org/10.1111/brv.12544>, 2019.
- Hetzer, J., Forrest, M., Ribalaygua, J., Prado-López, C., and Hickler, T.: The fire weather in Europe: large-scale trends towards higher danger, *Environmental Research Letters*, 19, 084017, <https://doi.org/10.1088/1748-9326/ad5b09>, 2024.
- Hopkins, W. J. and Faulkner, H.: To The RescEU? Disaster Response As A Driver For European Integration, Tech. rep., University of Canterbury, 2021.
- Hundhausen, M., Feldmann, H., Kohlhepp, R., and Pinto, J. G.: Climate change signals of extreme precipitation return levels for Germany in a transient convection-permitting simulation ensemble, *International Journal of Climatology*, 44, 1454–1471, <https://doi.org/10.1002/joc.8393>, 2024.
- Jacob, D., Elizalde, A., Haensler, A., Hagemann, S., Kumar, P., Podzun, R., Rechid, D., Remedio, A. R., Saeed, F., Sieck, K., Teichmann, C., and Wilhelm, C.: Assessing the Transferability of the Regional Climate Model REMO to Different COordinated Regional Climate Downscaling EXperiment (CORDEX) Regions, *Atmosphere*, 3, 181–199, <https://doi.org/10.3390/atmos3010181>, 2012.
- Jacob, D., Petersen, J., Eggert, B., Alias, A., Christensen, O. B., Bouwer, L. M., Braun, A., Colette, A., Déqué, M., Georgievski, G., Georgopoulou, E., Gobiet, A., Menut, L., Nikulin, G., Haensler, A., Hempelmann, N., Jones, C., Keuler, K., Kovats, S., Kröner, N., Kotlarski, S., Kriegsmann, A., Martin, E., van Meijgaard, E., Moseley, C., Pfeifer, S., Preuschmann, S., Radermacher, C., Radtke, K., Rechid, D.,



- Rounsevell, M., Samuelsson, P., Somot, S., Soussana, J.-F., Teichmann, C., Valentini, R., Vautard, R., Weber, B., and Yiou, P.: EURO-CORDEX: new high-resolution climate change projections for European impact research, *Regional Environmental Change*, 14, 563–578, <https://doi.org/10.1007/s10113-013-0499-2>, 2014.
- 725 Jain, P., Castellanos-Acuna, D., Coogan, S. C. P., Abatzoglou, J. T., and Flannigan, M. D.: Observed increases in extreme fire weather driven by atmospheric humidity and temperature, *Nature Climate Change*, 12, 63–70, <https://doi.org/10.1038/s41558-021-01224-1>, 2022.
- James, R., Washington, R., Schleussner, C.-F., Rogelj, J., and Conway, D.: Characterizing half-a-degree difference: a review of methods for identifying regional climate responses to global warming targets, *WIREs Climate Change*, 8, e457, <https://doi.org/10.1002/wcc.457>, 2017.
- Jolly, W. M., Cochrane, M. A., Freeborn, P. H., Holden, Z. A., Brown, T. J., Williamson, G. J., and Bowman, D. M. J. S.: Climate-induced variations in global wildfire danger from 1979 to 2013, *Nature Communications*, 6, 7537, <https://doi.org/10.1038/ncomms8537>, 2015.
- 730 Jones, M. W., Abatzoglou, J. T., Veraverbeke, S., Andela, N., Lasslop, G., Forkel, M., Smith, A. J. P., Burton, C., Betts, R. A., van der Werf, G. R., Sitch, S., Canadell, J. G., Santín, C., Kolden, C., Doerr, S. H., and Le Quéré, C.: Global and Regional Trends and Drivers of Fire Under Climate Change, *Reviews of Geophysics*, 60, e2020RG000 726, <https://doi.org/10.1029/2020RG000726>, 2022.
- Jones, M. W., Veraverbeke, S., Andela, N., Doerr, S. H., Kolden, C., Mataveli, G., Pettinari, M. L., Quéré, C. L., Rosan, T. M., Werf, G. R. v. d., Wees, D. v., and Abatzoglou, J. T.: Global rise in forest fire emissions linked to climate change in the extratropics, *Science*, 386, <https://doi.org/10.1126/science.adl5889>, 2024.
- 735 Jones, P. W.: First- and Second-Order Conservative Remapping Schemes for Grids in Spherical Coordinates, *Monthly Weather Review*, 127, 2204–2210, [https://doi.org/10.1175/1520-0493\(1999\)127<2204:FASOCR>2.0.CO;2](https://doi.org/10.1175/1520-0493(1999)127<2204:FASOCR>2.0.CO;2), 1999.
- Katragkou, E., Sobolowski, S. P., Teichmann, C., Solmon, F., Pavlidis, V., Rechid, D., Hoffmann, P., Fernandez, J., Nikulin, G., and Jacob, D.: Delivering an Improved Framework for the New Generation of CMIP6-Driven EURO-CORDEX Regional Climate Simulations, *Bulletin of the American Meteorological Society*, 105, E962–E974, <https://doi.org/10.1175/BAMS-D-23-0131.1>, 2024.
- 740 Kendall, M. G.: Rank correlation methods., Hafner Publishing Co., Griffin, 1955.
- Kjellström, E., Barring, L., Nikulin, G., Nilsson, C., Persson, G., and Strandberg, G.: Production and use of regional climate model projections – A Swedish perspective on building climate services, *Climate Services*, 2-3, 15–29, <https://doi.org/10.1016/j.cliser.2016.06.004>, 2016.
- 745 Kreider, M. R., Higuera, P. E., Parks, S. A., Rice, W. L., White, N., and Larson, A. J.: Fire suppression makes wildfires more severe and accentuates impacts of climate change and fuel accumulation, *Nature Communications*, 15, 2412, <https://doi.org/10.1038/s41467-024-46702-0>, 2024.
- Kudláčková, L., Bartošová, L., Linda, R., Bláhová, M., Poděbradská, M., Fischer, M., Balek, J., Žalud, Z., and Trnka, M.: Assessing fire danger classes and extreme thresholds of the Canadian Fire Weather Index across global environmental zones: a review, *Environmental Research Letters*, 20, 013 001, <https://doi.org/10.1088/1748-9326/ad97cf>, 2024.
- 750 Lehner, F., Nadeem, I., and Formayer, H.: Evaluating skills and issues of quantile-based bias adjustment for climate change scenarios, *Advances in Statistical Climatology, Meteorology and Oceanography*, 9, 29–44, <https://doi.org/10.5194/ascmo-9-29-2023>, 2023.
- Mann, H. B.: Nonparametric Tests Against Trend, *Econometrica*, 13, 245–259, <https://doi.org/10.2307/1907187>, 1945.
- Maraun, D.: Bias Correcting Climate Change Simulations - a Critical Review, *Current Climate Change Reports*, 2, 211–220, <https://doi.org/10.1007/s40641-016-0050-x>, 2016.
- 755 Maraun, D. and Widmann, M.: Cross-validation of bias-corrected climate simulations is misleading, *Hydrology and Earth System Sciences*, 22, 4867–4873, <https://doi.org/10.5194/hess-22-4867-2018>, 2018.



- Maraun, D., Shepherd, T. G., Widmann, M., Zappa, G., Walton, D., Gutiérrez, J. M., Hagemann, S., Richter, I., Soares, P. M. M., Hall, A., and Mearns, L. O.: Towards process-informed bias correction of climate change simulations, *Nature Climate Change*, 7, 764–773, <https://doi.org/10.1038/nclimate3418>, 2017.
- Masson-Delmotte, V., Zhai, P., Pirani, A., Connors, S. L., Péan, C., Berger, S., Caud, N., Chen, Y., Goldfarb, L., Gomis, M. I., Huang, M., Leitzell, K., Lonnoy, E., Matthews, J. B. R., Maycock, T. K., Waterfield, T., Yelekçi, , Yu, R., and Zhou, B., eds.: *Climate Change 2021: The Physical Science Basis. Contribution of Working Group I to the Sixth Assessment Report of the Intergovernmental Panel on Climate Change*, Cambridge University Press, Cambridge, United Kingdom and New York, NY, USA, <https://doi.org/10.1017/9781009157896>, 2021.
- McElhinny, M., Beckers, J. F., Hanes, C., Flannigan, M., and Jain, P.: A high-resolution reanalysis of global fire weather from 1979 to 2018 – overwintering the Drought Code, *Earth System Science Data*, 12, 1823–1833, <https://doi.org/10.5194/essd-12-1823-2020>, 2020.
- Meijgaard, E. v., Ulft, L. H. v., Lenderink, G., Roode, S. R. d., Wipfler, E. L., Boers, R., and Timmermans, R. M. A. v.: Refinement and application of a regional atmospheric model for climate scenario calculations of Western Europe, KVR, ISBN 978-90-8815-046-3, 2012.
- Miller, J., Böhnisch, A., Ludwig, R., and Brunner, M. I.: Climate change impacts on regional fire weather in heterogeneous landscapes of central Europe, *Natural Hazards and Earth System Sciences*, 24, 411–428, <https://doi.org/10.5194/nhess-24-411-2024>, 2024.
- Moemken, J., Koerner, B., Ehmele, F., Feldmann, H., and Pinto, J. G.: Recurrence of Drought Events Over Iberia. Part II: Future Changes Using Regional Climate Projections, *Tellus A: Dynamic Meteorology and Oceanography*, 74, 262–279, <https://doi.org/10.16993/tellusa.52>, 2022.
- Moreira, F., Ascoli, D., Safford, H., Adams, M. A., Moreno, J. M., Pereira, J. M. C., Catry, F. X., Armesto, J., Bond, W., González, M. E., Curt, T., Koutsias, N., McCaw, L., Price, O., Pausas, J. G., Rigolot, E., Stephens, S., Tavsanoglu, C., Vallejo, V. R., Van Wilgen, B. W., Xanthopoulos, G., and Fernandes, P. M.: Wildfire management in Mediterranean-type regions: paradigm change needed, *Environmental Research Letters*, 15, 011 001, <https://doi.org/10.1088/1748-9326/ab541e>, 2020.
- Mozny, M., Trnka, M., and Brázdil, R.: Climate change driven changes of vegetation fires in the Czech Republic, *Theoretical and Applied Climatology*, 143, 691–699, <https://doi.org/10.1007/s00704-020-03443-6>, 2021.
- Muerth, M. J., Gauvin St-Denis, B., Ricard, S., Velázquez, J. A., Schmid, J., Minville, M., Caya, D., Chaumont, D., Ludwig, R., and Turcotte, R.: On the need for bias correction in regional climate scenarios to assess climate change impacts on river runoff, *Hydrology and Earth System Sciences*, 17, 1189–1204, <https://doi.org/10.5194/hess-17-1189-2013>, 2013.
- Muñoz-Sabater, J., Dutra, E., Agustí-Panareda, A., Albergel, C., Arduini, G., Balsamo, G., Boussetta, S., Choulga, M., Harrigan, S., Hersbach, H., Martens, B., Miralles, D. G., Piles, M., Rodríguez-Fernández, N. J., Zsoter, E., Buontempo, C., and Thépaut, J.-N.: ERA5-Land: a state-of-the-art global reanalysis dataset for land applications, *Earth System Science Data*, 13, 4349–4383, <https://doi.org/10.5194/essd-13-4349-2021>, 2021.
- Parisien, M.-A., Barber, Q. E., Hirsch, K. G., Stockdale, C. A., Erni, S., Wang, X., Arseneault, D., and Parks, S. A.: Fire deficit increases wildfire risk for many communities in the Canadian boreal forest, *Nature Communications*, 11, 2121, <https://doi.org/10.1038/s41467-020-15961-y>, 2020.
- Pausas, J. G. and Keeley, J. E.: Wildfires and global change, *Frontiers in Ecology and the Environment*, 19, 387–395, <https://doi.org/10.1002/fee.2359>, 2021.
- Pfeifer, S., Bülow, K., Gobiet, A., Hänsler, A., Mudelsee, M., Otto, J., Rechid, D., Teichmann, C., and Jacob, D.: Robustness of Ensemble Climate Projections Analyzed with Climate Signal Maps: Seasonal and Extreme Precipitation for Germany, *Atmosphere*, 6, 677–698, <https://doi.org/10.3390/atmos6050677>, 2015.



- Podur, J. and Wotton, M.: Will climate change overwhelm fire management capacity?, *Ecological Modelling*, 221, 1301–1309, <https://doi.org/10.1016/j.ecolmodel.2010.01.013>, 2010.
- Quilcaille, Y., Batibeniz, F., Ribeiro, A. F. S., Padrón, R. S., and Seneviratne, S. I.: Fire weather index data under historical and shared socioeconomic pathway projections in the 6th phase of the Coupled Model Intercomparison Project from 1850 to 2100, *Earth System Science Data*, 15, 2153–2177, <https://doi.org/10.5194/essd-15-2153-2023>, 2023.
- Ramos, A. M., Russo, A., DaCamara, C. C., Nunes, S., Sousa, P., Soares, P. M. M., Lima, M. M., Hurdud, A., and Trigo, R. M.: The compound event that triggered the destructive fires of October 2017 in Portugal, *iScience*, 26, 106 141, <https://doi.org/10.1016/j.isci.2023.106141>, 2023.
- Resco de Dios, V., Hedon, J., Cunill Camprubí, , Thapa, P., Martínez del Castillo, E., Martínez de Aragón, J., Bonet, J. A., Balaguer-Romano, R., Díaz-Sierra, R., Yebra, M., and Boer, M. M.: Climate change induced declines in fuel moisture may turn currently fire-free Pyrenean mountain forests into fire-prone ecosystems, *Science of The Total Environment*, 797, 149 104, <https://doi.org/10.1016/j.scitotenv.2021.149104>, 2021.
- Rovithakis, A., Grillakis, M. G., Seiradakis, K. D., Giannakopoulos, C., Karali, A., Field, R., Lazaridis, M., and Voulgarakis, A.: Future climate change impact on wildfire danger over the Mediterranean: the case of Greece, *Environmental Research Letters*, 17, 045 022, <https://doi.org/10.1088/1748-9326/ac5f94>, 2022.
- Ruffault, J., Curt, T., Moron, V., Trigo, R. M., Mouillot, F., Koutsias, N., Pimont, F., Martin-StPaul, N., Barbero, R., Dupuy, J.-L., Russo, A., and Belhadj-Khedher, C.: Increased likelihood of heat-induced large wildfires in the Mediterranean Basin, *Scientific Reports*, 10, 13 790, <https://doi.org/10.1038/s41598-020-70069-z>, 2020.
- San-Miguel-Ayanz, J., Schulte, E., Schmuck, G., Camia, A., Stobl, P., Liberta, G., Giovando, C., Boca, R., Sedano, F., Kempeneers, P., McInerney, D., Withmore, C., Oliveira, S. S. d., Rodrigues, M., Durrant, T., Corti, P., Oehler, F., Vilar, L., Amatulli, G., San-Miguel-Ayanz, J., Schulte, E., Schmuck, G., Camia, A., Stobl, P., Liberta, G., Giovando, C., Boca, R., Sedano, F., Kempeneers, P., McInerney, D., Withmore, C., Oliveira, S. S. d., Rodrigues, M., Durrant, T., Corti, P., Oehler, F., Vilar, L., and Amatulli, G.: Comprehensive Monitoring of Wildfires in Europe: The European Forest Fire Information System (EFFIS), in: *Approaches to Managing Disaster - Assessing Hazards, Emergencies and Disaster Impacts*, IntechOpen, ISBN 978-953-51-0294-6, 2012.
- Schumacher, D. L., Singh, J., Hauser, M., Fischer, E. M., Wild, M., and Seneviratne, S. I.: Exacerbated summer European warming not captured by climate models neglecting long-term aerosol changes, *Communications Earth & Environment*, 5, 182, <https://doi.org/10.1038/s43247-024-01332-8>, 2024.
- Schwertfeger, B. T., Lohmann, G., and Lipskoch, H.: Introduction of the BiasAdjustCXX command-line tool for the application of fast and efficient bias corrections in climatic research, *SoftwareX*, 22, 101 379, <https://doi.org/10.1016/j.softx.2023.101379>, 2023.
- Scott, A. C. and Glasspool, I. J.: The diversification of Paleozoic fire systems and fluctuations in atmospheric oxygen concentration, *Proceedings of the National Academy of Sciences*, 103, 10 861–10 865, <https://doi.org/10.1073/pnas.0604090103>, 2006.
- Seager, R., Hooks, A., Williams, A. P., Cook, B., Nakamura, J., and Henderson, N.: Climatology, Variability, and Trends in the U.S. Vapor Pressure Deficit, an Important Fire-Related Meteorological Quantity, *Journal of Applied Meteorology and Climatology*, 54, 1121–1141, <https://doi.org/10.1175/JAMC-D-14-0321.1>, 2015.
- Sen, P. K.: Estimates of the Regression Coefficient Based on Kendall’s Tau, *Journal of the American Statistical Association*, 63, 1379–1389, <https://doi.org/10.1080/01621459.1968.10480934>, 1968.
- Shepherd, T. G.: Atmospheric circulation as a source of uncertainty in climate change projections, *Nature Geoscience*, 7, 703–708, <https://doi.org/10.1038/ngeo2253>, 2014.



- Sørland, S. L., Brogli, R., Pothapakula, P. K., Russo, E., Van de Walle, J., Ahrens, B., Anders, I., Buchignani, E., Davin, E. L., Demory, M.-E., Dosio, A., Feldmann, H., Früh, B., Geyer, B., Keuler, K., Lee, D., Li, D., van Lipzig, N. P. M., Min, S.-K., Panitz, H.-J., Rockel, B., Schär, C., Steger, C., and Thiery, W.: COSMO-CLM regional climate simulations in the Coordinated Regional Climate Downscaling Experiment (CORDEX) framework: a review, *Geoscientific Model Development*, 14, 5125–5154, <https://doi.org/10.5194/gmd-14-5125-2021>, 2021.
- Taylor, K. E., Stouffer, R. J., and Meehl, G. A.: An Overview of CMIP5 and the Experiment Design, *Bulletin of the American Meteorological Society*, 93, 485–498, <https://doi.org/10.1175/BAMS-D-11-00094.1>, 2012.
- Teichmann, C., Bülow, K., Otto, J., Pfeifer, S., Rechid, D., Sieck, K., and Jacob, D.: Avoiding Extremes: Benefits of Staying below +1.5 °C Compared to +2.0 °C and +3.0 °C Global Warming, *Atmosphere*, 9, 115, <https://doi.org/10.3390/atmos9040115>, 2018.
- Teutschbein, C. and Seibert, J.: Bias correction of regional climate model simulations for hydrological climate-change impact studies: Review and evaluation of different methods, *Journal of Hydrology*, 456–457, 12–29, <https://doi.org/10.1016/j.jhydrol.2012.05.052>, 2012.
- Theil, H.: A Rank-Invariant Method of Linear and Polynomial Regression Analysis, in: *Henri Theil's Contributions to Economics and Econometrics: Econometric Theory and Methodology*, edited by Raj, B. and Koerts, J., pp. 345–381, Springer Netherlands, Dordrecht, ISBN 978-94-011-2546-8, 1950.
- Tinker, J., Lowe, J., Holt, J., Pardaens, A., and Wiltshire, A.: Validation of an ensemble modelling system for climate projections for the northwest European shelf seas, *Progress in Oceanography*, 138, 211–237, <https://doi.org/10.1016/j.pocan.2015.07.002>, 2015.
- Tong, Y., Gao, X., Han, Z., Xu, Y., Xu, Y., and Giorgi, F.: Bias correction of temperature and precipitation over China for RCM simulations using the QM and QDM methods, *Climate Dynamics*, 57, 1425–1443, <https://doi.org/10.1007/s00382-020-05447-4>, 2021.
- Turco, M., Bedia, J., Liberto, F. D., Fiorucci, P., Hardenberg, J. v., Koutsias, N., Llasat, M.-C., Xystrakis, F., and Provenzale, A.: Decreasing Fires in Mediterranean Europe, *PLOS ONE*, 11, e0150663, <https://doi.org/10.1371/journal.pone.0150663>, 2016.
- Urbieto, I. R., Zavala, G., Bedia, J., Gutiérrez, J. M., Miguel-Ayanz, J. S., Camia, A., Keeley, J. E., and Moreno, J. M.: Fire activity as a function of fire–weather seasonal severity and antecedent climate across spatial scales in southern Europe and Pacific western USA, *Environmental Research Letters*, 10, 114013, <https://doi.org/10.1088/1748-9326/10/11/114013>, 2015.
- Van de Velde, J., Demuzere, M., De Baets, B., and Verhoest, N. E. C.: Exploring the Effect of Occurrence-Bias-Adjustment Assumptions on Hydrological Impact Modeling, *Water*, 13, 1573, <https://doi.org/10.3390/w13111573>, 2021.
- van der Werf, G. R., Randerson, J. T., Giglio, L., van Leeuwen, T. T., Chen, Y., Rogers, B. M., Mu, M., van Marle, M. J. E., Morton, D. C., Collatz, G. J., Yokelson, R. J., and Kasibhatla, P. S.: Global fire emissions estimates during 1997–2016, *Earth System Science Data*, 9, 697–720, <https://doi.org/10.5194/essd-9-697-2017>, 2017.
- Van Wagner, C.: Development and structure of the Canadian Forest Fire Weather Index System, Technical Report 35, The Canadian Forestry Service, Ottawa, 1987.
- Varela, V., Vlachogiannis, D., Sfetsos, A., Karozis, S., Politi, N., and Giroud, F.: Projection of Forest Fire Danger due to Climate Change in the French Mediterranean Region, *Sustainability*, 11, 4284, <https://doi.org/10.3390/su11164284>, 2019.
- Vautard, R., Gobiet, A., Jacob, D., Belda, M., Colette, A., Déqué, M., Fernández, J., García-Díez, M., Goergen, K., Güttler, I., Halenka, T., Karacostas, T., Katragkou, E., Keuler, K., Kotlarski, S., Mayer, S., van Meijgaard, E., Nikulin, G., Patarčić, M., Scinocca, J., Sobolowski, S., Suklitsch, M., Teichmann, C., Warrach-Sagi, K., Wulfmeyer, V., and Yiou, P.: The simulation of European heat waves from an ensemble of regional climate models within the EURO-CORDEX project, *Climate Dynamics*, 41, 2555–2575, <https://doi.org/10.1007/s00382-013-1714-z>, 2013.



- Vautard, R., Gobiet, A., Sobolowski, S., Kjellström, E., Stegehuis, A., Watkiss, P., Mendlik, T., Landgren, O., Nikulin, G., Teichmann, C., and Jacob, D.: The European climate under a 2 °C global warming, *Environmental Research Letters*, 9, 034 006, <https://doi.org/10.1088/1748-9326/9/3/034006>, 2014.
- Vautard, R., Kadygrov, N., Iles, C., Boberg, F., Buonomo, E., Bülow, K., Coppola, E., Corre, L., Meijgaard, E. v., Nogherotto, R., Sandstad, M., Schwingshackl, C., Somot, S., Aalbers, E., Christensen, O. B., Ciarlo, J. M., Demory, M.-E., Giorgi, F., Jacob, D., Jones, R. G., Keuler, K., Kjellström, E., Lenderink, G., Levavasseur, G., Nikulin, G., Sillmann, J., Solidoro, C., Sørland, S. L., Steger, C., Teichmann, C., Warrach-Sagi, K., and Wulfmeyer, V.: Evaluation of the Large EURO-CORDEX Regional Climate Model Ensemble, *Journal of Geophysical Research: Atmospheres*, 126, e2019JD032 344, <https://doi.org/10.1029/2019JD032344>, 2021.
- Viegas, D. X., Bovio, G., Ferreira, A., Nosenzo, A., and Sol, B.: Comparative study of various methods of fire danger evaluation in southern Europe, *International Journal of Wildland Fire*, 9, 235–246, <https://doi.org/10.1071/wf00015>, 1999.
- Voltaire, A., Sanchez-Gomez, E., Salas y Méliá, D., Decharme, B., Cassou, C., Sénési, S., Valcke, S., Beau, I., Alias, A., Chevallier, M., Déqué, M., Deshayes, J., Douville, H., Fernandez, E., Madec, G., Maisonnave, E., Moine, M.-P., Planton, S., Saint-Martin, D., Szopa, S., Tyteca, S., Alkama, R., Belamari, S., Braun, A., Coquart, L., and Chauvin, F.: The CNRM-CM5.1 global climate model: description and basic evaluation, *Climate Dynamics*, 40, 2091–2121, <https://doi.org/10.1007/s00382-011-1259-y>, 2013.
- Vrac, M., Noël, T., and Vautard, R.: Bias correction of precipitation through Singularity Stochastic Removal: Because occurrences matter, *Journal of Geophysical Research: Atmospheres*, 121, 5237–5258, <https://doi.org/10.1002/2015JD024511>, 2016.
- Wehrli, K., Guillo, B. P., Hauser, M., Leclair, M., and Seneviratne, S. I.: Assessing the Dynamic Versus Thermodynamic Origin of Climate Model Biases, *Geophysical Research Letters*, 45, 8471–8479, <https://doi.org/10.1029/2018GL079220>, <https://onlinelibrary.wiley.com/doi/pdf/10.1029/2018GL079220>, 2018.
- Williams, A. P., Abatzoglou, J. T., Gershunov, A., Guzman-Morales, J., Bishop, D. A., Balch, J. K., and Lettenmaier, D. P.: Observed Impacts of Anthropogenic Climate Change on Wildfire in California, *Earth's Future*, 7, 892–910, <https://doi.org/10.1029/2019EF001210>, 2019.
- Wotton, B. M.: Interpreting and using outputs from the Canadian Forest Fire Danger Rating System in research applications, *Environmental and Ecological Statistics*, 16, 107–131, <https://doi.org/10.1007/s10651-007-0084-2>, 2009.
- Wotton, B. M. and Flannigan, M. D.: Length of the fire season in a changing climate, *The Forestry Chronicle*, 69, 187–192, <https://doi.org/10.5558/tfc69187-2>, 1993.
- Xavier, A. C. F., Martins, L. L., Rudke, A. P., de Moraes, M. V. B., Martins, J. A., and Blain, G. C.: Evaluation of Quantile Delta Mapping as a bias-correction method in maximum rainfall dataset from downscaled models in São Paulo state (Brazil), *International Journal of Climatology*, 42, 175–190, <https://doi.org/10.1002/joc.7238>, 2022.
- Zheng, B., Ciais, P., Chevallier, F., Chuvieco, E., Chen, Y., and Yang, H.: Increasing forest fire emissions despite the decline in global burned area, *Science Advances*, 7, <https://doi.org/10.1126/sciadv.abh2646>, 2021.
- Zscheischler, J., Fischer, E. M., and Lange, S.: The effect of univariate bias adjustment on multivariate hazard estimates, *Earth System Dynamics*, 10, 31–43, <https://doi.org/10.5194/esd-10-31-2019>, 2019.